

Distinct types of theta rhythmicity are induced by social and fearful stimuli in a network associated with social memory

Alex Tendler and Shlomo Wagner,

Sagol Department of Neurobiology, University of Haifa, Haifa, Israel

Corresponding Author: Shlomo Wagner, Sagol Department of Neurobiology, Faculty of Natural Sciences University of Haifa, Mt. Carmel, Haifa, Israel 31905. Tel: (+972)-4-8288773, Fax: +(972)-4-8288763, Email: shlomow@research.haifa.ac.il

Competing interest statement: None of the authors has any financial and non-financial competing interest in the data presented in this paper.

Abstract	18
Rhythmic activity in the theta range is thought to promote neuronal communication	19
between brain regions. Here we performed chronic telemetric recordings in socially	20
behaving rats to monitor electrophysiological activity in limbic brain regions linked to	21
social behavior. Social encounters were associated with increased rhythmicity in the	22
high theta range (7-10 Hz) that was proportional to the stimulus degree of novelty.	23
This modulation of theta rhythmicity, which was specific for social stimuli, appeared	24
to reflect a brain-state of social arousal. In contrast, the same network responded to a	25
fearful stimulus by enhancement of rhythmicity in the low theta range (3-7 Hz).	26
Moreover, theta rhythmicity showed different pattern of coherence between the	27
distinct brain regions in response to social and fearful stimuli. We suggest that the two	28
types of stimuli induce distinct arousal states that elicit different patterns of theta	29
rhythmicity, which cause the same brain areas to communicate in different modes.	30
	31
	32

Introduction	33
Oscillatory brain activity, mostly categorized to the theta (3-12 Hz), beta (12-30 Hz)	34
and gamma (30-80 Hz) bands, is thought to coordinate neural activity in vast neuronal	35
assemblies dispersed over different brain regions (1). This type of coordination may	36
underlie high level cognitive functions, such as speech and social communication (2,	37
3) that are impaired in autism spectrum disorders (ASD) (4). Increasing evidence	38
suggest that individuals with ASD show deficits in long-range neuronal	39
communication associated with low-frequency rhythms, such as the theta rhythm (5-	40
7). Nonetheless, a clear connection between rhythmic brain activity and social	41
behavior has not yet been established.	42
Mammalian social organization depends on the ability to recognize and remember	43
individual conspecifics (8). This social recognition memory (SRM) can be assessed in	44
rodents using their innate tendency to investigate novel conspecifics more persistently	45
than familiar ones (9). In the SRM habituation-dishabituation test, social memory is	46
assessed by the gradual reduction in the amount of time the animal spends	47
investigating a particular social stimulus during consecutive encounters (10). This	48
short-term memory was shown to be mediated mainly by chemical cues	49
(semiochemicals) perceived via the main and accessory olfactory systems (11). Upon	50
binding of semiochemicals to the receptors expressed by the sensory neurons of the	51
main olfactory epithelium and the vomeronasal organ, sensory information is	52
conveyed to the main (MOB) and accessory (AOB) olfactory bulbs, respectively (12).	53
Both bulbs then project, directly and indirectly, to the medial amygdala (MeA) (13,	54
14) that is thought to transfer the information to the hippocampus through the lateral	55
septum (LS) (15). The MOB projects also to several cortical areas comprising the	56

primary olfactory cortex, of which the piriform cortex (Pir) is best characterized (16)	57
(Figure 1).	58
Here we hypothesized that social behavior is associated with an elevation of rhythmic	59
activity in the network of brain areas that process social stimuli. To examine this	60
hypothesis we recorded electrophysiological activity from the brains of freely-	61
behaving adult male rats performing the SRM paradigm (Supplementary Video 1). A	62
telemetric system was used to record from wire electrodes chronically implanted in	63
the five aforementioned brain regions: MOB, AOB, MeA, LS and Pir (12). We found	64
that social encounters were associated with enhancement of brain rhythmic activity,	65
specifically at 7-10 Hz range, in all brain regions. This enhancement that was	66
proportional to the degree of novelty of the social stimulus appeared to reflect an	67
internal brain-state associated with social arousal. In contrast, a fear-conditioned tone,	68
which is associated with fear arousal, induced rhythmicity in the low theta range (3-7	69
Hz) in the same network of brain regions. Moreover, social and fearful stimuli elicited	70
different patterns of change in coherence between the distinct brain regions. We	71
hypothesize that these two types of stimuli induce distinct arousal states in the animal,	72
which are reflected by the different kinds of theta rhythmicity. We further suggest that	73
the distinct types of theta rhythmicity support different modes of communication	74
between the various brain areas. These in turn may modify cognitive processes such	75
as memory acquisition and recall depending on the value and saliency of the stimulus	76
by enhancing synchronous neuronal activity between remote neuronal assemblies.	77
	78
Results	79
Brain theta rhythmicity is modulated by the novelty of the social stimulus	80

Electrophysiological recordings were carried out in the brains of freely-behaving adult male rats performing the SRM habituation-dishabituation paradigm (Figure 2a). We first analyzed the dynamics of the local field potential (LFP) in the course of the behavioral paradigm. A highly rhythmic LFP was recorded in all brain areas during social encounters (Figure 2b). Power spectral density (PSD) analysis of the LFP showed a prominent peak at ~8 Hz, typical for the high theta band (1), in all areas (Figure 2c). The value of this peak, termed theta power (TP), was very low in the absence of a social stimulus (Base, Figure 2d-e) but increased profoundly during the first encounter (Enc. 1). It then gradually decreased during further encounters with the same stimulus (Enc. 2-4), but increased again when another novel stimulus was introduced (Enc. 5). These changes in theta power during SRM testing closely followed the changes in investigation time (IT) (Figure 2f), with both parameters appearing to correlate with the degree of stimulus novelty.

We next analyzed the effect of social and non-social stimuli on the dynamics of investigation time and theta power in all recorded brain areas. As exemplified in Figure 3a (lower panel), exposure of an animal to either type of stimulus caused similar dynamics of the investigation time. However, there was a vast difference with regards to the theta power response to the social and non-social stimuli: whereas significant theta power modulation that was similar across all brain regions was observed with social stimuli, whether awake or anesthetized, object and odor stimuli did not cause such an effect (Figure 3a, upper panels).

Combined analyses of the modulation of both theta power and investigation time in animals exposed to social and object stimuli are presented in Figure 3b. Social stimuli caused a marked increase of mean theta power during Enc. 1 compared to Base, with the MOB and AOB showing the largest changes (6.2 dB/Hz) and other areas showing

more moderate ones (4.0-5.1 dB/Hz). In all regions tested, the theta power decreased 106
gradually during the habituation phase (Enc. 1-4) but returned the values obtained in 107
Enc. 1 after dishabituation (Enc. 5) ($p < 0.005$ One-way repeated measures ANOVA, * 108
 $p_{\text{corr}} < 0.05$ *post-hoc* paired t-test, Figure 3 – source data 1-2). In contrast, object stimuli 109
elicited a much weaker initial change from Base to Enc. 1 (1.1-2.7 dB/Hz) in all brain 110
regions. Furthermore, the theta power showed modulation during the object paradigm 111
similarly to the social paradigm only in the MOB, and even this change was not 112
statistically significant ($p > 0.05$, Figure 3 – source data 1). In a sharp contrast to the 113
theta power, comparison of the investigation time of social and object paradigms 114
showed a highly similar course and magnitude of habituation and dishabituation that 115
were statistically significant in both cases (Figure 3c, Figure 3 – source data 1-2). 116
Taken together, these results show that in almost all recorded brain areas, theta power 117
is modulated by the degree of novelty of social but not object stimuli. 118

The modulation of theta rhythmicity during social encounters is driven by an 119 internal brain-state of arousal 120

The lack of theta power modulation despite the clear investigation time modulation 121
induced by object stimuli rejects the possibility that the theta rhythmicity is caused by 122
the investigative behavior. We therefore reasoned that rather, theta power modulation 123
may reflect processes that are either directly driven by the sensory input (Bottom-Up 124
processes) or induced by an internal state of the brain that is modulated by the 125
saliency of the social stimulus (Top-Down processes). In order to distinguish between 126
these two possibilities, we continued our recordings for 5 minutes after the stimulus 127
was removed from the arena (Post 1-5). As depicted in Figure 4a, the theta 128
rhythmicity did not cease with the removal of the social stimulus following Enc. 1, 129
but remained at a high level during most of the Post 1 period (for spectrograms of the 130

full experiment see Figure 4 – figure supplements 1-5). Plotting the mean
instantaneous theta power as a function of time, revealed that this was true for all
encounters with a social stimulus. In contrast, encounters with object stimuli were
followed by a sharp drop in the theta power to a low level almost immediately
following stimulus removal (Figure 4b, for all other brain areas see Figure 4 – figure
supplements 6-7). This significant reduction in mean theta power between the Enc.
and Post periods of the object paradigm was characteristic of all brain areas (Figure
4c, * $p < 0.05$ paired t-test, Figure 4 – source data 1). In contrast, high theta power
levels were found in both these periods in the social paradigm ($p > 0.05$). Moreover, all
encounters with social stimuli showed a steep but gradual increase in theta power
during the first 15 s in which the stimulus was being transferred into the arena (Figure
4a, d, gray bars). This rise in theta power probably reflects the subject's anticipation
for a social meeting, as there was no similar increase with object stimuli (Figure 4d).
Altogether, these data suggest that the changes in theta power during the SRM test
reflect a graded internal brain-state of arousal that is proportional to the novelty of the
social stimulus and slowly fades away after its removal.

**The theta rhythmicity during social behavior emerges from multiple sources
with dynamic coherence between brain areas**

The theta rhythmicity recorded in the network may reflect a single rhythm originating
from one source. In that case, the various brain regions are expected to display high
correlation and similar dynamics of coherence in their rhythmicity. Alternatively, if it
represents a combination of multiple independent rhythms arising from several
sources, we expect low correlation and differential dynamics of coherence between
various brain regions. To discriminate between these possibilities, we first examined
the cross-correlation of the LFP, filtered in the theta range, between the MeA and the

other brain areas. Despite the fact that both areas are directly connected to the MeA, the strongest correlation appeared with the LS, and the weakest with the MOB (Figure 5a-d). Moreover, whereas the correlation between the MeA and LS was significantly higher during Enc. 1 (blue) compared to Base (red), the MOB showed consistently low correlation with the MeA during both periods. The presence of a social stimulus thus appears to differentially affect the correlation of theta rhythmicity between distinct brain areas.

We next analyzed the coherence of the LFP signal among all brain areas during the Base, Enc. 1 and Post 1 periods of the SRM paradigm. As depicted in Figure 6a, the coherence between the MeA and the LS showed several prominent peaks, especially in the theta and gamma bands. Yet, while no change was recorded in the gamma band, the theta coherence showed a significant increase between the Base and Enc. 1. Furthermore, similarly to theta rhythmicity itself (Figure 4), the high coherence at theta range persisted during the Post 1 period despite the lack of a social stimulus (Figure 6a,c). In contrast, the coherence in theta band between the MeA and MOB remained low throughout all periods (Figure 6b,c). Analyses across all regions revealed a hierarchy in the theta coherence between the MeA and all other areas, ranging from a low level with the MOB and AOB, medium coherence with the Pir and high coherence with the LS (Figure 6d). This notion of functional hierarchy between brain regions is strengthened by the fact that despite their largest physical distance, the highest level of theta coherence was found between the MeAs in the two hemispheres (Figure 6 – figure supplements 1 and 3). Furthermore, the theta coherence between the MeA and the higher brain centers (Pir, LS) significantly increased during Enc. 1 and Post 1 (* $p_{\text{corr}} < 0.05$, paired t-test, Figure 6 – source data 1), while no change was recorded between the MeA and both areas of the olfactory

bulb (MOB, AOB, $p_{\text{corr}} > 0.05$). This suggests the existence of at least two independent
theta rhythms, one that governs the olfactory bulb and another that dominates higher
brain structures. This conclusion is further supported by the findings that the MOB
shows opposite relationships with all other brain areas; high coherence with the AOB
and low coherence with the higher areas (Figure 6e, Figure 6 – figure supplements 2
and 3). Moreover, a significant enhancement in theta coherence with the AOB was
observed during Enc. 1 and Post1 (* $p_{\text{corr}} < 0.05$, paired t-test, Figure 6 – source data
1), while all other regions showed no change ($p_{\text{corr}} > 0.05$, paired t-test). Interestingly,
similar enhancement of theta coherence between the AOB and MOB was recorded
with object stimuli, while these stimuli did not cause any enhancement of the
coherence between the MeA and LS or Pir (Figure 6f,g, Figure 6 – source data 1.
Together these data support multiple sources of theta rhythmicity in the network.

**Distinct types of theta rhythmicity are induced in the same brain regions by
social and fearful stimuli**

Theta rhythmicity was previously found to be elicited in several brain regions during
states of arousal, mainly in response to fearful stimuli (17). This phenomenon was
best studied in the context of fear learning in a network of brain regions comprising
the basolateral complex of the amygdala (lateral and basolateral amygdala),
hippocampus and medial prefrontal cortex (18). In this network, a recall of a fearful
memory, induced by a fear-conditioned stimulus, elicits robust theta rhythmicity that
shows high coherence between these brain regions (19-23). Here we examined
whether the brain state-induced theta rhythmicity during the SRM paradigm is similar
to the fear-induced rhythmicity. To address this question we compared the theta
rhythmicity induced by a social encounter to that of a fear stimulus within the social
network that we investigated. To that end, a new cohort of six animals was implanted

with wire electrodes as before, with an additional electrode in the nucleus accumbens (NAcc), which was recently shown to be involved in social motivation (24, 25). These animals were fear-conditioned by coupling a 40 s-long tone to an electrical foot shock for five consecutive times separated by 180 s intervals (Figure. 7 – figure supplement 1a). A day later the electrical activity was recorded in two consecutive sessions, each following a 30 min of habituation to the arena. The first session was recorded during a recall of fear memory (FC experiment), and the second during a 5-min long encounter with a novel social stimulus (SR experiment). During the FC experiments (Figure. 7 – figure supplement 1b), introduction of the fear-conditioned tone caused animals to begin moving intensively, followed by immobility (freezing) towards the end of the tone, in anticipation of the foot shock. The freezing response was especially significant at the end of the first tone (Figure. 7 – figure supplement 1c). Thus, the fear-conditioned tone caused a robust arousal state that was associated with intense movement of the conditioned animals. We then compared the theta rhythmicity between the FC and SR experiments. A PSD analysis of the LFP signals recorded in the LS during 5 minutes prior to stimulus introduction (Base) yielded a similar profile in both cases (Figure 7a, red). However, the PSD was very different between the two types of stimuli during the first 15 s following stimulus introduction (Figure 7a, blue). Whereas the fear stimulus showed a marked peak at the low theta range (3-7 Hz), the social stimulus resulted in a peak at the high theta range (7-10 Hz). This change is clearly observed when subtracting the Base PSD from the stimulus profile (Figure 7b). These differences appeared in all recorded brain regions (Figure 7c) and Statistical analysis showed a highly significant interaction between the type of experiment (FC or SR) and theta band (Figure 7d) (** $p < 0.01$, two-way repeated measures ANOVA, Figure 7 – source data 1). Thus, we conclude that fearful and

social stimuli cause changes in very different ranges of theta rhythmicity in the same	231
limbic network of brain regions. We suggest that these different types of theta	232
rhythmicity reflect distinct arousal states; the low theta reflects aversive arousal that is	233
associated with fear while the high theta reflects appetitive arousal associated with a	234
social encounter.	235
Distinct changes in coherence are induced in the network by social and fearful	236
stimuli	237
We next examined how the coherence between the various brain regions changes in	238
response to the two types of arousing stimuli. Figures 8a depicts the coherence	239
between the MeA and LS during Base and stimulus periods of FC and SR	240
experiments, respectively. The change in coherence of the two stimuli is presented in	241
Figure 8b and reveals a positive peak at the high theta range for the social encounter,	242
and at the low theta range for the fear memory recall. A quantitative analysis of all	243
coherence changes within the network in both ranges showed that this tendency	244
generally holds for all pairs of brain regions (Figure 8c). Accordingly, most pairs	245
showed a statistically significant interaction between the type of experiment (FC or	246
SR) and theta band (high or low) (* $p < 0.05$, ** $p < 0.01$, two-way repeated measures	247
ANOVA, Figure 8 – source data 1). Nevertheless, the magnitude of changes was	248
different between distinct pairs. For example, the changes in the coherence between	249
the LS and NAcc were much smaller than those recorded between the Pir and NAcc	250
and did not show any statistical significance. Moreover, the increases of coherence	251
between the AOB-MOB and MOB-Pir pairs were much bigger in SR compared to the	252
FC experiment. We conclude that the distinct arousal states are characterized by	253
distinct patterns of coherence changes within that same network of brain regions	254
(Figure 9).	255

	256
Discussion	257
This study demonstrates that an encounter with a social stimulus causes increased	258
LFP rhythmicity in the high theta range (7-10 Hz), in a network of limbic brain areas	259
associated with social memory. Strikingly, the change in theta rhythmicity is directly	260
proportional to the novelty of the social partner, and may thus be considered a	261
neuronal correlate of short-term social memory (26). Since the modulation of theta	262
rhythmicity is observed even when anesthetized stimuli are used, we infer that it does	263
not depend on the behavior of the social stimulus. Despite the similarity in	264
investigative behavior, such modulation of theta rhythmicity is not observed with	265
object stimuli, suggesting that it is social-specific. Since the augmented theta	266
rhythmicity and the associated increase in theta coherence persist beyond the removal	267
of the social stimulus itself, we conclude that these parameters do not mirror sensory	268
inputs but rather reflect a state of arousal that slowly fades away. This is in agreement	269
with the fact that the increase in theta power occurs prior to the actual introduction of	270
the social stimulus in the arena, suggesting increased arousal due to the anticipated	271
social encounter. Finally, since the change in theta rhythmicity during the SRM test	272
correlates with the novelty of the social stimulus, we posit that it reflects a graded	273
level of arousal, which is proportional to the stimulus saliency.	274
One of the questions that arise from the study is whether the social encounter-induced	275
state of arousal is elicited by the "social" quality of the stimulus or whether it simply	276
results from the complexity of the stimulus. Notably, the social stimulus is much more	277
complex than the single object or odor stimuli that we used as controls. It emits a	278
complex mixture of odors and semiochemicals, and in addition to the main and	279
accessory olfactory systems it also stimulates the visual, auditory and somatosensory	280

systems. It is not likely that the full complexity of the social stimulus may be 281

mimicked by the use of any artificial mixture of odors, hence the possibility that the 282

arousal state results from the complexity of the stimulus cannot be excluded. On the 283

other hand, at least as regards to fear-associated arousal, it is well documented (27) 284

that a very simple cue is sufficient to evoke a state of arousal, such that is observed by 285

the freezing of rodents in response to the pure odorant 2,3,5-Trimethyl-3-thiazoline 286

(TMT), a component of fox odor (28), or to a pure tone in a fear conditioning 287

paradigm (29). This suggests that the factor that determines the state of arousal is not 288

the complexity of the stimulus but rather the information it embodies with regards to 289

the natural environment of the animal. 290

Many studies, both in animals and humans, have linked brain theta rhythmicity to the 291

processing of emotional cues (30-37). In animals theta rhythmicity was mostly studied 292

in the hippocampus (38), where it was classified into two types, Type 1 and Type 2. 293

The atropine-insensitive Type 1 theta rhythmicity shows higher frequency (8-12 Hz) 294

and is thought to be associated mainly with voluntary movement. In contrast, 295

atropine-sensitive Type 2 rhythmicity is characterized by lower frequency (4-8 Hz) 296

and is thought to be linked to arousal during states of immobility (39, 40). Notably, 297

Type 2 rhythmicity was mostly studied using states of fear and aversive stimuli and 298

was shown to be induced by neutral stimuli if conditioned by fear or introduced in the 299

presence of predators (35-37). The relationship of the two types of hippocampal theta 300

rhythmicity and similar rhythms recorded from other brain regions, such as in our 301

case, should be cautiously examined for several reasons. First, recent studies showed 302

that in the hippocampus itself there are differences in the profile of theta rhythmicity 303

between the earlier studied dorsal hippocampus and the more recently studied ventral 304

hippocampus (41), the latter of which shows theta rhythmicity with stronger 305

association to the one recoded in the mPFC (42), and may be dissociated from the
 dorsal hippocampus under certain conditions such as decision making (43). Second,
 even for the dorsal hippocampus the dichotomy between the two types of theta
 rhythmicity is far from being perfect with Type 2 rhythmicity reported to reach 12 Hz
 at some states and Type 1 rhythmicity reported to disappear during certain movements
 (40). Interestingly, researchers reported that in cats the correlation between movement
 and Type 1 rhythmicity was good at the beginning of the experiments, when a lot of
 exploratory and object manipulation behavior was observed, but deteriorated towards
 the end of the experiments, when the animals were still moving but were uninterested
 in the task (40). This might suggest that in the hippocampus too, high frequency Type
 1 theta may be associated with sensory information processing during "positive"
 arousal states associated with motivational voluntary movements, such as
 exploration, while low frequency Type 2 theta may be linked to "negative" arousal
 states, such as those caused by fear, which is usually associated with freezing.
 Regardless of the nature of hippocampal theta oscillations, theta rhythmicity
 associated with emotional states was reported in several other brain areas (44-46). Of
 particular interest is the finding that theta rhythmicity in a limbic network that
 includes the hippocampus, medial prefrontal cortex and the basolateral complex of the
 amygdala (lateral and basolateral amygdala) is associated with fear memories.
 Importantly, the consolidation and recall of long-term fear memory was found to be
 associated with elevated coherence of the theta rhythmicity in this network (19, 20,
 22, 23, 47), while its extinction was associated with a decline in coherence, in a brain-
 region dependent manner (48). Moreover, interfering with theta coherence through
 local electrical micro-stimulation affected fear-memory recall and extinction
 depending on theta phase (47). Thus, coordinated arousal-induced theta rhythmicity

within this network seems to be involved in consolidation and recall of aversive 331
 memories (22, 47). Here we demonstrated for the first time that similar phenomena 332
 occur in a distinct network of limbic areas that are linked to social memory, in the 333
 course of social encounters. Importantly, a comparison of the theta activity between 334
 social and fearful stimuli revealed that although both cause a state of arousal, the 335
 patterns of theta rhythmicity and coherence within the same network are completely 336
 different. First, in agreement with previous studies (19, 20, 22, 23, 47), the recall of 337
 fear memory causes rhythmicity in the low theta range, while a social encounter 338
 elicits rhythmic activity in the high theta range. This suggests the existence of two 339
 types of arousal: fear-associated arousal and social related arousal. Second, each of 340
 these conditions caused a distinct pattern of coherence changes between the same 341
 regions of the network. Given these results we hypothesize that the distinct types of 342
 theta rhythmicity promote different communication protocols (49) for the 343
 coordination of neural activity in the network, which depend on the emotional state of 344
 the animal. Our results are in agreement with the hypothesis that theta rhythmicity 345
 facilitates cognitive processes such as memory formation that are associated with 346
 emotionally salient stimuli (50). 347

The source and distribution of theta rhythms in the mammalian brain are not fully 348
 understood (46). This issue was extensively studied in the hippocampus (38), which 349
 was shown have the capacity to self-generate theta rhythmicity (51). Yet, as described 350
 above theta rhythmicity also exists in various cortical and limbic areas, where it 351
 shows dynamic coherence with the hippocampal theta rhythm. One area shown to 352
 display robust theta rhythmicity is the olfactory bulb, where it follows the rhythm of 353
 respiration ("sniff cycle") (52). Sniffing, similarly to whisking, is a sensory sampling 354
 activity, the rate of which dynamically changes throughout the theta band and is 355

strongly influenced by internal arousal and motivational state of the animal (53, 54). 356

Specifically, high-frequency sniffing (8-12 Hz) develops in anticipation of reward 357

delivery (55-58). The olfactory bulb theta rhythm and sniffing are not usually 358

coherent with the hippocampal rhythm. However, in some odor-based learning tasks 359

these rhythms do become transiently coherent (59-61), a process that was suggested to 360

be mediated by cholinergic neurons in the medial septum (62). Interestingly, whisking 361

was shown to get occasionally phase locked with the sniff cycle (63, 64) or with the 362

hippocampal theta rhythm (65) during exploratory behavior. Thus, various generators 363

of theta rhythmicity in the brain, such as those reflected by sniffing, whisking or the 364

hippocampal theta rhythm may become dynamically coupled by the brain 365

neuromodulatory systems. While we did not monitor sniffing in our experiments, 366

several recent studies reported changes in sniffing during both social interactions (66, 367

67) and fear conditioning (68). These studies showed that the sniff cycle adopt high- 368

range theta rhythmicity during social interactions, and low-range rhythmicity during 369

fear conditioning. These differences are probably reflected by the distinct rates of 370

theta rhythmicity that we record in the MOB and AOB during these conditions. This 371

may explain our observation of high coherence between MOB-AOB and the low 372

coherence each of them display with all other regions. Moreover, while the coherence 373

between the MOB-AOB is increased during exploration of both social and object 374

stimuli, the coherence between the LS –MeA increases only during social 375

interactions. Thus, the theta rhythmicity displayed by the AOB and MOB probably 376

emerges from a distinct generator, most likely the sniff cycle, that is separate from the 377

one causing rhythmicity in higher brain areas. Furthermore, the significant differences 378

in correlation and coherence dynamics between the various limbic areas suggest the 379

involvement of distinct generators as well. For example, neither paradigm showed 380

significant coherence changes between the LS-NAcc, as opposed to a significant 381
increase in coherence between the LS -MeA or LS-Pir during social interactions. It 382
should be noted that these differences cannot not be accounted for by local diffusion 383
of LFP signals, since the LS is much closer to the NAcc than to the MeA or Pir. 384
Direct synaptic connections cannot explain these differences either as the MeA shows 385
very low coherence with the AOB, despite the strong bidirectional connections 386
between them, but rather displays the highest coherence with the contralateral MeA, 387
despite the lack of direct synaptic pathway (69). Therefore, the differential coherence 388
changes between distinct pairs of brain regions during the various conditions are most 389
likely mediated by either a common input to these regions or via brain-region specific 390
neuromodulatory systems. However, the arousal-driven modulation of theta 391
rhythmicity which seems to be common to all brain regions is probably mediated by a 392
general, brain-wide neuromodulatory mechanism such as neurohormonal activity (70, 393
71). 394
An ever growing body of evidence implies rhythmic brain activity in various 395
cognitive processes, particularly in memory acquisition and recall (72-74). 396
Specifically, slow frequency rhythms such as the theta rhythm, are hypothesized to 397
mediate communication between brain regions and to promote the temporal binding 398
of neural assemblies in these areas into coherent networks subserving specific 399
cognitive processes (1, 74-76). During the last decade, several prominent theories 400
implied a disordered or weak communication among brain regions as a major deficit 401
underlying ASD etiology and symptoms (3, 5, 7, 77, 78). Indeed, multiple recent 402
studies found reduction in the power and coherence of slow brain rhythms, such as the 403
alpha and theta rhythms, in ASD individuals (79-85). In agreement with these 404
findings, our results suggest that arousal-driven theta rhythmicity may help bind 405

correlated neuronal assemblies in distinct brain areas participating in cognitive and 406
emotional processes underlying social behavior. A disruption of the correlated 407
neuronal activity associated with the theta rhythmicity is likely to impair these 408
processes (3, 5, 72) resulting in atypical social behaviors. 409
410

<u>Materials and methods:</u>	411
Animals	412
Sprague-Dawley (SD) male rats (5– 6 weeks of age, 250–300 gr) served as subjects	413
while SD or Wistar Holo/Hannover male rats (5– 6 weeks of age, 250–300 gr) served	414
as stimuli. All rats were purchased from Harlan Laboratories (Jerusalem, Israel) and	415
housed in groups (2-5 per cage) in the SPF rat facility of the University of Haifa under	416
veterinary supervision, food and water available <i>ad libitum</i> , lights on between 7:00 –	417
19:00. Experiments were performed in a strict accordance with the guidelines of the	418
University of Haifa and approved by its Animal Care and Use Committee.	419
Electrodes	420
We used home-made electrodes for implantation. Stimulating electrodes were	421
prepared by twisting together two stainless steel wires (A-M Systems, Sequim, WA,	422
USA) with bare diameter of 0.005" (Coated-0.008"). Recording electrodes were	423
prepared from Tungsten wire (A-M Systems) with bare diameter of 0.008" (Coated-	424
0.011") soldered to stainless steel wire. For reference/ground wire we used stainless	425
steel wires attached to a small screw.	426
Surgery and electrodes implantation	427
The rats were anesthetized with subcutaneously injected Ketamine (10%	428
0.09cc/100gr) and Medetomidine (0.1% 0.055cc/100gr). Anesthesia level was	429
monitored by testing toe pinch reflexes and held constant throughout surgery with	430
consecutive injections. The body temperature of the rat was kept constant at	431
approximately 37°C, using a closed-loop temperature controller connected to a rectal	432
temperature probe and a heating-pad placed under the rat (FHC, Bowdoin, MA,	433
USA).	434

Anesthetized rats were fixed in a stereotaxic apparatus (Stoelting, Wood Dale, IL, 435
USA), with the head flat, the skin was gently removed and holes were drilled in the 436
skull for implantation of electrodes and for reference/ground screw connection. 437
Stimulating electrodes were placed in the left AOB (A/P= +3.0 mm, L/M= +1.0 mm, 438
D/V= -4.0 mm at 50 degrees) and MOB (A/P= +7.08 mm, L/M= +1.0 mm, D/V= -5.5 439
mm). Recording electrodes were placed in antero-ventral area of the MeA (A/P= -2.4 440
mm, L/M= +3.18 mm, D/V= -8.5 mm), LS (A/P= -0.24 mm, L/M= +0.4 mm, D/V= - 441
4.4 mm) and Pir (A/P= +3.2mm, L/M= +3.5mm, D/V=-5.5mm), as well as in the 442
NAcc (A/P= +1.2 mm, L/M= +1.4 mm, D/V= -5.8 mm) in later experiments. Each 443
electrode location was verified by its typical field potential signal, evoked in the MeA 444
and LS by AOB stimulation (86) and in the Pir by MOB stimulation (87). Following 445
verification implanted electrodes (one at a time) were fixed by dental cement 446
(Stoelting). When all electrodes were in place, the free ends of the stainless steel wires 447
(including one wire for each stimulation electrode) were wired up to a connector 448
which was then connected to the skull by dental cement, followed by skin is suturing. 449
To avoid a need of soldering, procedure that could damage brain tissue due to 450
excessive heat, we used gold pins inserted to the connector holes under pressure 451
which destroyed the wires isolation to create a contact between the wires and the pins. 452
After surgery, Amoxicilin (15%, 0.07cc/100gr) was injected daily (for three days) to 453
prevent contamination. Rats allowed recovery for at least 7 days before experiments. 454

The experimental setup 455

All experiments were video-recorded from above the arena (see Supplementary video 456
1) by a CCD camera (Prosilica GC1290 GigE, Allied Vision Technology, 457
Taschenweg, Germany). Electrophysiological recordings where made using an 8- 458
channel wireless recording system (W8, Multi Channel Systems, Reutlingen, 459

Germany). Recoded signals (sampled at 1 kHz, low-pass filtered at 0-300Hz) were
synchronized with the video recordings by start signal sent through a digital to USB
converter (NI USB-6008, National Instruments, Austin, TX, USA) controlled by a
self-written Labview program (National Instruments).

The experimental arena comprised a three-layer box (inner dimensions: width - 26
cm, length - 28 cm, height - 40 cm) with door on its front side. The inner layer was
made of material (cloth) stretched on cuboid metal carcass to soften mechanical
bumps of the recording system. The outer layer was made of adhesive black tape to
prevent light entrance. A stainless steel net serves as a faraday cage in between these
layers and the Multi-Channel wireless receiver was placed between it and the inner
layer. During the experiment the arena was illuminated by dim red light. We used a
double floor made of two plastic slices that can be separately removed.

Experiments

Overall, we recorded from 22 animals, of them 11 were tested with the social
paradigm, 6 with the object paradigm (1 animal was tested with both) and 6 animals
were tested with both fear conditioning and social encounter. Social recognition
memory using anesthetized stimuli was performed in two animals and smell
recognition was tested in three animals. The sample size is not always the same for all
brain regions since in some of the recorded animals we lost the signals from specific
electrodes due to various causes.

At the beginning of each experiment, the tested rat was taken out of its home cage and
the wireless transmitter was fastened to the connector on its head by a male-to-male
Interconnect header (Mill-Max Mfg. Oyster Bay, NY, USA) with 18 pins. Following
0.5-1 hour of habituation in the experimental arena, the rat was subjected to social,
object, smell recognition test (Figure 2a), or fear conditioning test (Figure. 7 – figure

supplement 1). Each encounter initiated by pressing "start" button on LabVIEW 485
virtual instrument that sends synchronizing start signal to the camera and the wireless 486
system. Then, during a period of 15 seconds, the stimulus was removed from its cage 487
and delivered into the experimental arena. At the end of each encounter following 488
stimulus removal, the upper floor slice is taken out and thoroughly cleaned with 70% 489
ethanol and water to remove any odors left by the stimulus. It was then put back 490
below the other slice 5 min after stimulus removal. 491

Stimuli 492

Rat stimuli were individually placed in clean covered plastic box and held in the 493
experiment room throughout the experiment. The two stimulus animals used for each 494
paradigm were always from different rat strains. Anesthetized animal stimuli were 495
subcutaneously injected Ketamine (10% 0.09cc/100gr) and Medetomidine (0.1% 496
0.055cc/100gr) 10 min prior to experiment. As object stimuli we used clean metal 497
office stapler and hole-puncher. For smell recognition we used small metal-net balls 498
filled with cloth soaked with artificial food smells of citrus and vanilla. The metal-net 499
ball was attached to the cage floor by hot melt adhesive. It should be noted that 500
abviously, both object and smell stimuli are much poorer sources of chemosignals that 501
social stimuli. 502

Fear Conditioning 503

Fear conditioning took place in a Plexiglas rodent conditioning chamber with a metal 504
grid floor dimly illuminated by a single house light and enclosed within a sound 505
attenuating chamber (Coulbourn Instruments, Lehigh Valley, PA, USA). Rats were 506
habituated to the chamber for 1 hour before fear conditioning. During fear 507
conditioning rats were presented with five pairings of a tone (CS; 40 s, 5 kHz, 75 dB) 508
that co-terminated with a foot-shock (US; 0.5 s, 1.3 mA). The inter-trial interval was 509

180 s. The fear recall experiments were conducted a day later in the experimental	510
arena described above, using the same procedure without the electrical foot shocks.	511
Histology	512
After completion of the experiments, the rats were anesthetized and killed with an	513
overdose of Isoflurane (Abbott Laboratories, Chicago, IL, USA). The brains are	514
removed and placed in PFA (4% in PBS) over night, followed by sectioning to 200	515
µm slices using vibrating slicer (Vibroslice, Campden Instruments, Lafayette, IN,	516
USA). The locations of the implanted electrode tips were identified using binocular	517
and compared to the Paxinos-Watson rat brain atlas (88).	518
Data analysis:	519
All analyses were done using self-written MATLAB programs (MathWorks, Natick,	520
MA, USA). In all cases when LFP signals were filtered we used band-pass filter	521
between 5-11 Hz (high theta band) using MATLAB 'fir1' function.	522
PSD estimation: We estimated Power Spectrum Density (PSD) of LFP signal using	523
multi-tapper approach based on standard Welch's method ('pwelch' function) using 1-s	524
long dpss (discrete prolate spheroidal sequences) window with 50% overlap. The peak	525
of the PSD curve was considered to be the maximum theta power value for each	526
encounter (Figure 2).	527
ΔTheta Power (ΔTP) calculation: For each brain region, the theta power obtained	528
during Enc. 0 (Base) was subtracted from the TP values of each encounter.	529
Spectrogram: For each brain region, spectrograms were computed for each rat per	530
trial using standard 'spectrogram' function with 1-s long dpss window with 50%	531
overlap.	532
LFP cross-correlation: We used standard 'xcorr' function with 'coeff' option for	533
cross-correlation between different brain regions of filtered LFP signals for each	534

second. The mean peak cross-correlation value across all 300 seconds of each 535
 encounter was considered to be the cross-correlation value of the encounter (Fig. 4a). 536

Coherence: The coherence between two signals x and y is defined as: 537

$$\text{Coh}_{xy}(f) = \frac{S_{xy}(f)}{\sqrt{S_{xx}(f)S_{yy}(f)}}$$

We computed the cross-spectrum $S_{xy}(f)$ and the auto-spectra of each signal $S_{xx}(f)$ 538
 and $S_{yy}(f)$ using the multitaper method (89), implemented in Chronux 2.0 (90), an 539
 open-source, data analysis toolbox available at <http://chronux.org>. Coherograms were 540
 computed using a moving window of 2 s shifted in 200 ms increments, 5 tapers, and 541
 time-bandwidth of 3. (params.tapers=[TW=3 K=5]; movingwin=[2 0.2];). As 542
 spectrograms, coherograms, for each brain region, were computed for each rat per trial. 543
 For each brain region, mean coherograms were obtained by averaging coherograms 544
 computed per trial across all rats. 545

Statistics 546

Statistical analyses were performed using MATLAB, except for repeated measures 547
 ANOVA analyses that were conducted using SPSS (IBM) statistical software. Each 548
 brain region was separately analyzed. Parametric t-test and ANOVA tests were used if 549
 data were found to be normally distributed (Lilliefors and Shapiro-Wilk tests). 550
 Bonferroni's corrections were performed for multiple comparisons using t-test. One- 551
 sided t-tests were used when a change in specific direction was expected before the 552
 experiment. 553

Acknowledgments 554

We thank Dr. Liza Barki-Harrington for a helpful reading of this manuscript. We 555
 thank Dr. Ido Izhaki and Ms. Rotem Gur for generous help with the statistical 556
 analyses. This research was supported by the Legacy Heritage Bio-Medical Program 557

of the Israel Science Foundation (grant #1901/08), by the Israel Science Foundation	558
(grant #1350/12) and by a Teva fellowship to A.T.	559
	560

References

	561
1. Buzsaki G, Draguhn A. Neuronal oscillations in cortical networks. <i>Science</i> . 2004;304(5679):1926-9.	562 563
2. Uhlhaas PJ, Pipa G, Lima B, Melloni L, Neuenschwander S, Nikolic D, et al. Neural synchrony in cortical networks: history, concept and current status. <i>Front Integr Neurosci</i> . 2009;3:17.	564 565 566
3. Uhlhaas PJ, Singer W. Neural synchrony in brain disorders: relevance for cognitive dysfunctions and pathophysiology. <i>Neuron</i> . 2006;52(1):155-68.	567 568
4. Geschwind DH. Advances in autism. <i>Annu Rev Med</i> . 2009;60:367-80.	569
5. Geschwind DH, Levitt P. Autism spectrum disorders: developmental disconnection syndromes. <i>Curr Opin Neurobiol</i> . 2007;17(1):103-11.	570 571
6. Rippon G, Brock J, Brown C, Boucher J. Disordered connectivity in the autistic brain: challenges for the "new psychophysiology". <i>International journal of psychophysiology : official journal of the International Organization of Psychophysiology</i> . 2007;63(2):164-72.	572 573 574
7. Wass S. Distortions and disconnections: disrupted brain connectivity in autism. <i>Brain Cogn</i> . 2011;75(1):18-28.	575 576
8. Wiley RH. Specificity and multiplicity in the recognition of individuals: implications for the evolution of social behaviour. <i>Biol Rev Camb Philos Soc</i> . 2013;88(1):179-95.	577 578
9. Gheusi G, Bluthé RM, Goodall G, Dantzer R. Social and individual recognition in rodents: Methodological aspects and neurobiological bases. <i>Behavioural processes</i> . 1994;33:59-88.	579 580 581
10. Ferguson JN, Young LJ, Insel TR. The neuroendocrine basis of social recognition. <i>Front Neuroendocrinol</i> . 2002;23(2):200-24.	582 583
11. Dulac C, Torello AT. Molecular detection of pheromone signals in mammals: from genes to behaviour. <i>Nature reviews Neuroscience</i> . 2003;4(7):551-62.	584 585

12. Dulac C, Wagner S. Genetic analysis of brain circuits underlying pheromone signaling.	586
Annu Rev Genet. 2006;40:449-67.	587
13. Kang N, Baum MJ, Cherry JA. Different profiles of main and accessory olfactory bulb	588
mitral/tufted cell projections revealed in mice using an anterograde tracer and a whole-	589
mount, flattened cortex preparation. Chemical senses. 2011;36(3):251-60.	590
14. Pro-Sistiaga P, Mohedano-Moriano A, Ubeda-Banon I, Del Mar Arroyo-Jimenez M,	591
Marcos P, Artacho-Perula E, et al. Convergence of olfactory and vomeronasal projections	592
in the rat basal telencephalon. J Comp Neurol. 2007;504(4):346-62.	593
15. Bielsky IF, Young LJ. Oxytocin, vasopressin, and social recognition in mammals. Peptides.	594
2004;25(9):1565-74.	595
16. Wilson DA, Sullivan RM. Cortical processing of odor objects. Neuron. 2011;72(4):506-19.	596
17. Knyazev GG. Motivation, emotion, and their inhibitory control mirrored in brain	597
oscillations. Neuroscience and biobehavioral reviews. 2007;31(3):377-95.	598
18. Pape HC, Pare D. Plastic synaptic networks of the amygdala for the acquisition,	599
expression, and extinction of conditioned fear. Physiological reviews. 2010;90(2):419-63.	600
19. Pape HC, Narayanan RT, Smid J, Stork O, Seidenbecher T. Theta activity in neurons and	601
networks of the amygdala related to long-term fear memory. Hippocampus.	602
2005;15(7):874-80.	603
20. Pare D, Collins DR. Neuronal correlates of fear in the lateral amygdala: multiple	604
extracellular recordings in conscious cats. The Journal of neuroscience : the official	605
journal of the Society for Neuroscience. 2000;20(7):2701-10.	606
21. Pare D, Collins DR, Pelletier JG. Amygdala oscillations and the consolidation of emotional	607
memories. Trends in cognitive sciences. 2002;6(7):306-14.	608
22. Popa D, Duvarci S, Popescu AT, Lena C, Pare D. Coherent amygdalocortical theta	609
promotes fear memory consolidation during paradoxical sleep. Proceedings of the	610
National Academy of Sciences of the United States of America. 2010;107(14):6516-9.	611

23.Seidenbecher T, Laxmi TR, Stork O, Pape HC. Amygdalar and hippocampal theta rhythm	612
synchronization during fear memory retrieval. Science. 2003;301(5634):846-50.	613
24.Dolen G, Darvishzadeh A, Huang KW, Malenka RC. Social reward requires coordinated	614
activity of nucleus accumbens oxytocin and serotonin. Nature. 2013;501(7466):179-84.	615
25.Gunaydin LA, Grosenick L, Finkelstein JC, Kauvar IV, Fenno LE, Adhikari A, et al. Natural	616
neural projection dynamics underlying social behavior. Cell. 2014;157(7):1535-51.	617
26.Liebe S, Hoerzer GM, Logothetis NK, Rainer G. Theta coupling between V4 and prefrontal	618
cortex predicts visual short-term memory performance. Nat Neurosci. 2012;15(3):456-62,	619
S1-2.	620
27.Takahashi LK, Chan MM, Pilar ML. Predator odor fear conditioning: current perspectives	621
and new directions. Neuroscience and biobehavioral reviews. 2008;32(7):1218-27.	622
28.Fendt M, Endres T, Apfelbach R. Temporary inactivation of the bed nucleus of the stria	623
terminalis but not of the amygdala blocks freezing induced by trimethylthiazoline, a	624
component of fox feces. The Journal of neuroscience : the official journal of the Society	625
for Neuroscience. 2003;23(1):23-8.	626
29.Rogan MT, Staubli UV, LeDoux JE. Fear conditioning induces associative long-term	627
potentiation in the amygdala. Nature. 1997;390(6660):604-7.	628
30.Aftanas LI, Varlamov AA, Pavlov SV, Makhnev VP, Reva NV. Affective picture processing:	629
event-related synchronization within individually defined human theta band is modulated	630
by valence dimension. Neuroscience letters. 2001;303(2):115-8.	631
31.Balconi M, Pozzoli U. Arousal effect on emotional face comprehension: frequency band	632
changes in different time intervals. Physiology & behavior. 2009;97(3-4):455-62.	633
32.Knyazev GG, Slobodskoj-Plusnin JY, Bocharov AV. Event-related delta and theta	634
synchronization during explicit and implicit emotion processing. Neuroscience.	635
2009;164(4):1588-600.	636

33.Luo Q, Cheng X, Holroyd T, Xu D, Carver F, Blair RJ. Theta band activity in response to	637
emotional expressions and its relationship with gamma band activity as revealed by MEG	638
and advanced beamformer source imaging. <i>Frontiers in human neuroscience</i> .	639
2013;7:940.	640
34.Maratos FA, Mogg K, Bradley BP, Rippon G, Senior C. Coarse threat images reveal theta	641
oscillations in the amygdala: a magnetoencephalography study. <i>Cognitive, affective &</i>	642
<i>behavioral neuroscience</i> . 2009;9(2):133-43.	643
35.Sainsbury RS, Harris JL, Rowland GL. Sensitization and hippocampal type 2 theta in the	644
rat. <i>Physiology & behavior</i> . 1987;41(5):489-93.	645
36.Sainsbury RS, Heynen A, Montoya CP. Behavioral correlates of hippocampal type 2 theta	646
in the rat. <i>Physiology & behavior</i> . 1987;39(4):513-9.	647
37.Sainsbury RS, Montoya CP. The relationship between type 2 theta and behavior.	648
<i>Physiology & behavior</i> . 1984;33(4):621-6.	649
38.Buzsaki G. Theta oscillations in the hippocampus. <i>Neuron</i> . 2002;33(3):325-40.	650
39.Bland BH. The physiology and pharmacology of hippocampal formation theta rhythms.	651
<i>Prog Neurobiol</i> . 1986;26(1):1-54.	652
40.Sainsbury RS. Hippocampal theta: a sensory-inhibition theory of function. <i>Neuroscience</i>	653
and biobehavioral reviews. 1998;22(2):237-41.	654
41.Adhikari A, Topiwala MA, Gordon JA. Synchronized Activity between the Ventral	655
Hippocampus and the Medial Prefrontal Cortex during Anxiety. <i>Neuron</i> . 2010;65(2):257-	656
69.	657
42.Jacinto LR, Reis JS, Dias NS, Cerqueira JJ, Correia JH, Sousa N. Stress affects theta activity	658
in limbic networks and impairs novelty-induced exploration and familiarization. <i>Frontiers</i>	659
in behavioral neuroscience. 2013;7:127.	660

43.Schmidt B, Hinman JR, Jacobson TK, Szkudlarek E, Argraves M, Escabi MA, et al.	661
Dissociation between Dorsal and Ventral Hippocampal Theta Oscillations during Decision-	662
Making. Journal of Neuroscience. 2013;33(14):6212-24.	663
44.Bland BH, Colom LV. Extrinsic and Intrinsic-Properties Underlying Oscillation and	664
Synchrony in Limbic Cortex. Prog Neurobiol. 1993;41(2):157-208.	665
45.Bland BH, Oddie SD. Theta band oscillation and synchrony in the hippocampal formation	666
and associated structures: the case for its role in sensorimotor integration. Behavioural	667
brain research. 2001;127(1-2):119-36.	668
46.Pignatelli M, Beyeler A, Leinekugel X. Neural circuits underlying the generation of theta	669
oscillations. Journal of physiology, Paris. 2012;106(3-4):81-92.	670
47.Lesting J, Daldrup T, Narayanan V, Himpe C, Seidenbecher T, Pape HC. Directional theta	671
coherence in prefrontal cortical to amygdalo-hippocampal pathways signals fear	672
extinction. PloS one. 2013;8(10):e77707.	673
48.Narayanan RT, Seidenbecher T, Kluge C, Bergado J, Stork O, Pape HC. Dissociated theta	674
phase synchronization in amygdalo- hippocampal circuits during various stages of fear	675
memory. The European journal of neuroscience. 2007;25(6):1823-31.	676
49.Kepecs A, Uchida N, Mainen ZF. The sniff as a unit of olfactory processing. Chemical	677
senses. 2006;31(2):167-79.	678
50.Pelletier JG, Pare D. Role of amygdala oscillations in the consolidation of emotional	679
memories. Biol Psychiatry. 2004;55(6):559-62.	680
51.Goutagny R, Jackson J, Williams S. Self-generated theta oscillations in the hippocampus.	681
Nat Neurosci. 2009;12(12):1491-3.	682
52.Rojas-Libano D, Frederick DE, Egana JI, Kay LM. The olfactory bulb theta rhythm follows	683
all frequencies of diaphragmatic respiration in the freely behaving rat. Frontiers in	684
behavioral neuroscience. 2014;8:214.	685

53.Chang FCT. Modification of Medullary Respiratory-Related Discharge Patterns by Behaviors and States of Arousal. Brain Res. 1992;571(2):281-92.	686
	687
54.Clarke S, Trowill JA. Sniffing and motivated behavior in the rat. Physiology & behavior. 1971;6(1):49-52.	688
	689
55.Freeman WJ, Viana Di Prisco G, Davis GW, Whitney TM. Conditioning of relative frequency of sniffing by rabbits to odors. Journal of comparative psychology. 1983;97(1):12-23.	690
	691
	692
56.Kepecs A, Uchida N, Mainen ZF. Rapid and precise control of sniffing during olfactory discrimination in rats. Journal of neurophysiology. 2007;98(1):205-13.	693
	694
57.Monod B, Mouly AM, Vigouroux M, Holley A. An investigation of some temporal aspects of olfactory coding with the model of multi-site electrical stimulation of the olfactory bulb in the rat. Behavioural brain research. 1989;33(1):51-63.	695
	696
	697
58.Wesson DW, Donahou TN, Johnson MO, Wachowiak M. Sniffing behavior of mice during performance in odor-guided tasks. Chemical senses. 2008;33(7):581-96.	698
	699
59.Kay LM. Theta oscillations and sensorimotor performance. Proceedings of the National Academy of Sciences of the United States of America. 2005;102(10):3863-8.	700
	701
60.Macrides F, Eichenbaum HB, Forbes WB. Temporal relationship between sniffing and the limbic theta rhythm during odor discrimination reversal learning. The Journal of neuroscience : the official journal of the Society for Neuroscience. 1982;2(12):1705-17.	702
	703
	704
61.Martin C, Beshel J, Kay LM. An olfacto-hippocampal network is dynamically involved in odor-discrimination learning. Journal of neurophysiology. 2007;98(4):2196-205.	705
	706
62.Tsanov M, Chah E, Reilly R, O'Mara SM. Respiratory cycle entrainment of septal neurons mediates the fast coupling of sniffing rate and hippocampal theta rhythm. The European journal of neuroscience. 2014;39(6):957-74.	707
	708
	709

63.Cao Y, Roy S, Sachdev RN, Heck DH. Dynamic correlation between whisking and breathing	710
rhythms in mice. The Journal of neuroscience : the official journal of the Society for	711
Neuroscience. 2012;32(5):1653-9.	712
64.Ranade S, Hangya B, Kepecs A. Multiple modes of phase locking between sniffing and	713
whisking during active exploration. The Journal of neuroscience : the official journal of	714
the Society for Neuroscience. 2013;33(19):8250-6.	715
65.Komisaruk BR. Synchrony between limbic system theta activity and rhythmical behavior	716
in rats. Journal of comparative and physiological psychology. 1970;70(3):482-92.	717
66.Assini R, Sirotin YB, Laplagne DA. Rapid triggering of vocalizations following social	718
interactions. Current biology : CB. 2013;23(22):R996-7.	719
67.Wesson DW. Sniffing behavior communicates social hierarchy. Current biology : CB.	720
2013;23(7):575-80.	721
68.Shionoya K, Hegoburu C, Brown BL, Sullivan RM, Doyere V, Mouly AM. It's time to fear!	722
Interval timing in odor fear conditioning in rats. Frontiers in behavioral neuroscience.	723
2013;7:128.	724
69.Canteras NS, Simerly RB, Swanson LW. Organization of projections from the medial	725
nucleus of the amygdala: a PHAL study in the rat. J Comp Neurol. 1995;360(2):213-45.	726
70.Lee SH, Dan Y. Neuromodulation of brain states. Neuron. 2012;76(1):209-22.	727
71.Marder E. Neuromodulation of neuronal circuits: back to the future. Neuron.	728
2012;76(1):1-11.	729
72.Buzsaki G, Watson BO. Brain rhythms and neural syntax: implications for efficient coding	730
of cognitive content and neuropsychiatric disease. Dialogues Clin Neurosci.	731
2012;14(4):345-67.	732
73.Cannon J, McCarthy MM, Lee S, Lee J, Borgers C, Whittington MA, et al. Neurosystems:	733
brain rhythms and cognitive processing. The European journal of neuroscience.	734
2014;39(5):705-19.	735

74.Fell J, Axmacher N. The role of phase synchronization in memory processes. Nature reviews Neuroscience. 2011;12(2):105-18.	736 737
75.Benchenane K, Tiesinga PH, Battaglia FP. Oscillations in the prefrontal cortex: a gateway to memory and attention. Curr Opin Neurobiol. 2011;21(3):475-85.	738 739
76.Jutras MJ, Buffalo EA. Synchronous neural activity and memory formation. Curr Opin Neurobiol. 2010;20(2):150-5.	740 741
77.Brock J, Brown CC, Boucher J, Rippon G. The temporal binding deficit hypothesis of autism. Development and psychopathology. 2002;14(2):209-24.	742 743
78.Kana RK, Libero LE, Moore MS. Disrupted cortical connectivity theory as an explanatory model for autism spectrum disorders. Phys Life Rev. 2011;8(4):410-37.	744 745
79.Barttfeld P, Amoruso L, Ais J, Cukier S, Bavassi L, Tomio A, et al. Organization of brain networks governed by long-range connections index autistic traits in the general population. Journal of neurodevelopmental disorders. 2013;5(1):16.	746 747 748
80.Coben R, Clarke AR, Hudspeth W, Barry RJ. EEG power and coherence in autistic spectrum disorder. Clinical neurophysiology : official journal of the International Federation of Clinical Neurophysiology. 2008;119(5):1002-9.	749 750 751
81.Doesburg SM, Vidal J, Taylor MJ. Reduced theta connectivity during set-shifting in children with autism. Frontiers in human neuroscience. 2013;7.	752 753
82.Isler JR, Martien KM, Grieve PG, Stark RI, Herbert MR. Reduced functional connectivity in visual evoked potentials in children with autism spectrum disorder. Clinical neurophysiology : official journal of the International Federation of Clinical Neurophysiology. 2010;121(12):2035-43.	754 755 756 757
83.Kikuchi M, Yoshimura Y, Hiraishi H, Munesue T, Hashimoto T, Tsubokawa T, et al. Reduced long-range functional connectivity in young children with autism spectrum disorder. Social cognitive and affective neuroscience. 2014.	758 759 760

84.Machado C, Estevez M, Leisman G, Melillo R, Rodriguez R, Defina P, et al. QEEG Spectral	761
and Coherence Assessment of Autistic Children in Three Different Experimental	762
Conditions. Journal of autism and developmental disorders. 2013.	763
85.Murias M, Webb SJ, Greenson J, Dawson G. Resting state cortical connectivity reflected in	764
EEG coherence in individuals with autism. Biol Psychiatry. 2007;62(3):270-3.	765
86.Gur R, Tendler A, Wagner S. Long-Term Social Recognition Memory Is Mediated by	766
Oxytocin-Dependent Synaptic Plasticity in the Medial Amygdala. Biol Psychiatry. 2014.	767
87.Cohen Y, Wilson DA, Barkai E. Differential Modifications of Synaptic Weights During Odor	768
Rule Learning: Dynamics of Interaction Between the Piriform Cortex with Lower and	769
Higher Brain Areas. Cerebral cortex. 2013.	770
88.Paxinos G, Watson C. The rat brain in stereotaxic coordinates. 6th ed. Amsterdam ;	771
Boston ;; Academic Press/Elsevier; 2007.	772
89.Thomson DJ. Spectrum Estimation and Harmonic-Analysis. P IEEE. 1982;70(9):1055-96.	773
90.Mitra P, Bokil H. Observed brain dynamics. Oxford ; New York: Oxford University Press;	774
2008. xxii, 381 p. p.	775
	776
	777

<u>Figures and tables</u>	778
Figure 1: A simplistic scheme of sensory information flow in the network of	779
brain regions thought to underlie social recognition memory.	780
Social olfactory cues are detected by sensory neurons in the main olfactory epithelium	781
(MOE) and vomeronasal organ (VNO). These neurons project to the main (MOB) and	782
accessory (AOB) olfactory bulbs, which transmit information, either directly or	783
indirectly (via the cortical nucleus of the amygdala – CoA) to the medial amygdala	784
(MeA). The MOB also innervates the piriform cortex (Pir). The MeA projects to the	785
lateral septum (LS), which innervates the hippocampus (Hip).	786
	787
Figure 2: Theta rhythmicity in the rat brain is enhanced during social	788
encounters, in correlation with the novelty of the social stimulus.	789
a) A scheme of the habituation-dishabituation SRM paradigm.	790
b) Examples of LFP traces recorded in the MOB, LS and MeA during a social	791
encounter.	792
c) Power spectral density (PSD) analyses of a 5-min LFP recording from all five	793
brain areas during a social encounter. Gray bar represents the 7-9 Hz band.	794
d) Superimposed PSD analyses of LFP recordings from the MeA of one animal	795
during the various stages of the SRM test.	796
e) As in d , zooming on the 4-10 Hz range.	797
f) The ~8 Hz PSD peak (TP) and social investigation time (IT) for the same	798
experiment as in d , plotted as a function of the encounter number. Encounter 0	799
represents no stimulus (Base).	800
	801

Figure 3: Theta rhythmicity is modulated by the novelty of social, but not other tested stimuli.

- a) TP for all brain areas (upper) as well as IT (lower) during the SRM test of one animal, using awake and anesthetized social stimuli as well as object and smell stimuli, all except smell tested with the same animal.
- b) Mean TP for the various brain regions averaged (\pm SEM) and plotted as a function of the test stage, for social (blue, n=8) and object (red, n=6) stimuli. A significant difference was found between the various encounters in all brain regions for social stimuli ($p < 0.005$, one-way repeated measures ANOVA, Figure 3 – source data 1a), while no difference was found for object recognition ($p > 0.05$, Figure 3 – source data 1b). *Post hoc* paired t-test showed significant differences between Enc. 1 and Enc. 4 as well as between Enc. 4 and Enc. 5 (dashed lines) in all brain regions for social stimuli (* $p_{\text{corr}} < 0.05$, Figure 3 – source data 2).
- c) As in **b**, for the IT of the social and object paradigms. Unlike the TP, both paradigms showed similarly significant modulation of the IT (Figure 3 – source data 1-2).

Figure 4: Modulation of the theta rhythmicity by social stimulus novelty reflects an internal state in the brain.

- a) Color-coded spectrograms of the LFP recorded in the MOB (upper), LS (middle) and MeA (lower) for 5 min before (Base), during (Enc. 1) and after (Post 1) the first encounter of the SRM test. All spectrograms are averages of five animals (4 animals for LS). Gray bar marks the 15 s needed for stimulus transfer to the arena.
- b) Upper – instantaneous Δ TP (change from mean Base) in the LS averaged over four rats (\pm SEM) during the Enc. and Post periods of all trials (1-5), for social (left,

- n=5) and object (right, n=4) paradigms. The 15 min breaks between last Post and next Enc. periods are labeled with gray bars. Lower – mean (\pm SEM) values for the corresponding periods shown above.
- c) Comparison of mean Δ TP averaged over all trials (1-5) for each brain area, between the Enc. and Post periods of the social and object paradigms (* $p < 0.05$, paired t-test, Figure 4 – source data 1).
- d) Left –the instantaneous Δ TP shown in **b**, expanded to show the initial 50 seconds of all encounters. Gray area represents the 15 s needed for stimulus transfer to the experimental arena. Right – Same for object stimuli.

Figure 5: Differential and dynamic correlation of theta rhythmicity between specific brain regions.

- a) Upper – superimposed LFP traces (filtered 5-11 Hz) from the MeA (black) and LS (colored) of one animal during Base (left, red) and Enc. 1 (right, blue). Lower – cross-correlations between both regions for each of the 300 seconds recorded during the same periods, with peaks labeled by colored dots.
- b) Same as **a** for the MeA and MOB.
- c) Middle – distribution of the cross-correlation peaks for the data in **a**. Borders – histograms of the cross-correlation peaks in the correlation (right) and lag (bottom) axes. Mean \pm SD are marked to the left (correlation) or above (lag) the histograms.
- d) Same as **c** for the data in **b**.

Figure 6: Theta coherence between specific brain regions increases during social encounter.

a) Mean (n=10 animals) coherence (0-100 Hz) of the LFP signals recorded in the MeA and LS during Base, Enc. 1 and Post 1 periods.	851
	852
b) Same animals, coherence analysis between the MeA and MOB.	853
c) Spectrograms (0-20 Hz) of the coherence analyses shown in a (between MeA and LS, upper panel) and b (between MeA and MOB, lower panel).	854
	855
d) Mean coherence at 8 Hz between the MeA and all other areas (MOB, AOB n=11; LS, Pir n=10) during the Base, Enc. 1 and Post 1 periods of social encounter (* $p_{\text{corr}} < 0.05$, paired t-test, Figure 5 – source data 1a).	856
	857
	858
e) Same as d , for coherence of the MOB with all other areas (* $p_{\text{corr}} < 0.05$, paired t-test, Figure 5 – source data 1b).	859
	860
f) Same as d , for object stimuli (Figure 5 – source data 1c).	861
g) Same as e , for object stimuli (* $p_{\text{corr}} < 0.05$, paired t-test, Figure 5 – source data 1d).	862
	863
Figure 7: Distinct types of theta rhythmicity are induced by social and fearful stimuli.	864
	865
a) PSD analyses (0-20 Hz) of LFP signal recorded in the LS of one animal, 5 min prior to stimulus introduction (Base, red) and 15 sec following it (Stimulus, blue) during fear memory recall (left, FC) and social encounter (right, SR).	866
	867
	868
b) The change between Stimulus and Base PSD analyses (Stimulus minus Base) shown in a , for FC and SR, superimposed.	869
	870
c) Mean change in PSD profile for all brain areas of the same six animals during the FC (continuous lines) and SR (dashed lines) experiments.	871
	872
d) Mean (\pm SEM) values of the peak change in PSD in the low (4-8 Hz, red and blue) and high (8-12 Hz, pink and light blue) theta ranges for the FC (red and pink) and	873
	874

SR (blue and light blue) experiments (** $p<0.01$, experiment X theta range	875
interaction, two-way repeated measures ANOVA, Figure 7 – source data 1).	876
	877
Figure 8: Distinct changes in theta coherence between various brain regions are	878
induced by social and fearful stimuli.	879
a) Coherence analyses (0-20 Hz) of LFP signal recorded in the LS and MeA of one	880
animal, 5 min prior to stimulus introduction (Base, red) and 15 sec following it	881
(Stimulus, blue) during fear memory recall (left, FC) and social encounter (right,	882
SR).	883
b) The change between Stimulus and Base coherence analyses (Stimulus minus Base)	884
shown in a , for FC and SR, superimposed.	885
c) Mean (\pm SEM) values of the peak change in coherence between all possible couples	886
of brain areas in the low (4-8 Hz, red and blue) and high (8-12 Hz, pink and light	887
blue) theta ranges for the FC (red and pink) and SR (blue and light blue)	888
experiments (* $p<0.05$, ** $p<0.01$, experiment X theta range interaction, two-way	889
repeated measures ANOVA, Figure 8 – source data 1).	890
	891
Figure 9: Different patterns of coherence change characterize the distinct	892
arousal states.	893
Graphical color-coded presentation of the mean changes in coherence for the FC and	894
SR experiments.	895
	896
Supplementary Video 1: Social encounter between two adult male rats in the	897
experimental arena. The recorded subject carries a black transmitter equipped with a	898
flashing led light of its head. Frame number is shown in the right low corner. The	899

graph below the movie shows the LFP recorded in the AOB (blue), MOB (red) and 900
MeA (green). The bottom graph shows raster plots of spikes detected from the 901
recorded multi-unit activity signal. 902
903
904

<u>Supplemental figures titles and legends</u>	905
	906
Figure 4 – figure supplement 1: Mean LFP spectrograms across the SRM paradigm for the AOB	907
	908
Color-coded spectrograms (0-20 Hz) of the LFP recorded in the AOB during the SRM test. Gray bar marks the 15 s needed for stimulus delivery to the arena. Mean of 5 animals.	909
	910
	911
	912
Figure 4 – figure supplement 2: Mean LFP spectrograms across the SRM paradigm for the MOB	913
	914
Color-coded spectrograms (0-20 Hz) of the LFP recorded in the MOB during the SRM test. Gray bar marks the 15 s needed for stimulus delivery to the arena. Mean of 5 animals.	915
	916
	917
	918
Figure 4 – figure supplement 3: Mean LFP spectrograms across the SRM paradigm for the MEA	919
	920
Color-coded spectrograms (0-20 Hz) of the LFP recorded in the MEA during the SRM test. Gray bar marks the 15 s needed for stimulus delivery to the arena. Mean of 5 animals.	921
	922
	923
	924
Figure 4 – figure supplement 4: Mean LFP spectrograms across the SRM paradigm for the LS	925
	926
Color-coded spectrograms (0-20 Hz) of the LFP recorded in the LS during the SRM test. Gray bar marks the 15 s needed for stimulus delivery to the arena. Mean of 4 animals.	927
	928
	929

	930
Figure 4 – figure supplement 5: Mean LFP spectrograms across the SRM	931
paradigm for the Pir	932
Color-coded spectrograms (0-20 Hz) of the LFP recorded in the Pir during the SRM	933
test. Gray bar marks the 15 s needed for stimulus delivery to the arena. Mean of 5	934
animals.	935
	936
Figure 4 – figure supplement 6: Comparison of mean instantaneous TP between	937
social and object stimuli, for the AOB and MOB	938
Upper panels – instantaneous Δ TP (change from mean Base) in each brain area	939
averaged over all animals (mean \pm SEM) during the Enc. and Post periods of all trials	940
(1-5), for social (left, n=5 rats) and object (right, n=4 rats) paradigms. The 15 min	941
breaks between last Post and next Enc. periods are labeled with gray bars. Lower	942
panels – mean (\pm SEM) values for the corresponding periods shown above.	943
	944
Figure 4 – figure supplement 7: Comparison of mean instantaneous TP between	945
social and object stimuli, for the MeA and Pir	946
Upper panels – instantaneous Δ TP (change from mean Base) in each brain area	947
averaged over all animals (mean \pm SEM) during the Enc. and Post periods of all trials	948
(1-5), for social (left, n=5 rats) and object (right, n=4 rats) paradigms. The 15 min	949
breaks between last Post and next Enc. periods are labeled with gray bars. Lower	950
panels – mean (\pm SEM) values for the corresponding periods shown above.	951
	952
Figure 6 – figure supplement 1: Mean spectrograms of coherence between the	953
MeA and all other areas during trial 1 of the SRM paradigm	954

Color-coded spectrograms (0-20 Hz) of the mean LFP coherence (MOB, AOB - n=11; LS, Pir - n=10, cMeA - contralateral MeA, n=3) between the MOB and all other brain areas, during the first trial of SRM test, each depicting continuous 15 min divided to the Base, Enc. 1 and Post 1 periods.

Figure 6 – figure supplement 2: Mean spectrograms of coherence between the MOB and all other areas during trial 1 of the SRM paradigm

Color-coded spectrograms (0-20 Hz) of the mean LFP coherence (MeA, AOB - n=11; LS, Pir - n=10, cMeA - contralateral MeA, n=3) between the MOB and all other brain areas, during the first trial of SRM test, each depicting continuous 15 min divided to the Base, Enc. 1 and Post 1 periods.

Figure 6 – figure supplement 3: Mean theta coherence during trial 1 of the SRM paradigm

a) Mean coherence at 8 Hz between the MeA and all other areas (MOB, AOB n=11; LS, Pir n=10, cMeA - contralateral MeA, n=3) during the Base, Enc. 1 and Post 1 periods of the SRM paradigm.

b) Same as **a**, for coherence of the MOB with all other areas.

Figure 7 – figure supplement 1: Arousal-driven locomotion during recall of fear memory

a) A schematic drawing of the fear conditioning session, comprising 5 events of 40-sec tone (gray bar) followed by brief electrical foot shock (red bar).

b) Locomotion activity of one animal during the recall of fear memory, one day after fear conditioning, plotted as a function of the experimental stage. Gray bars

represent the 40-sec long tone. Tone start is marked on the X-axis by T1...5 and 980

tone end by S1...5. 981

c) Mean locomotion (n=6 animals) during fear recall around the first tone, as a 982

function of time. Tone started 15 sec from beginning of the experiment and is 983

marked by a gray bar. Note the intense locomotion of the animals during most of 984

the tone, as opposed to their freezing at the end of it, when expecting the electrical 985

foot shock. Black dashed line represent the 15-sec period during which theta 986

activity was calculated. Error bars represent SEM. 987

988

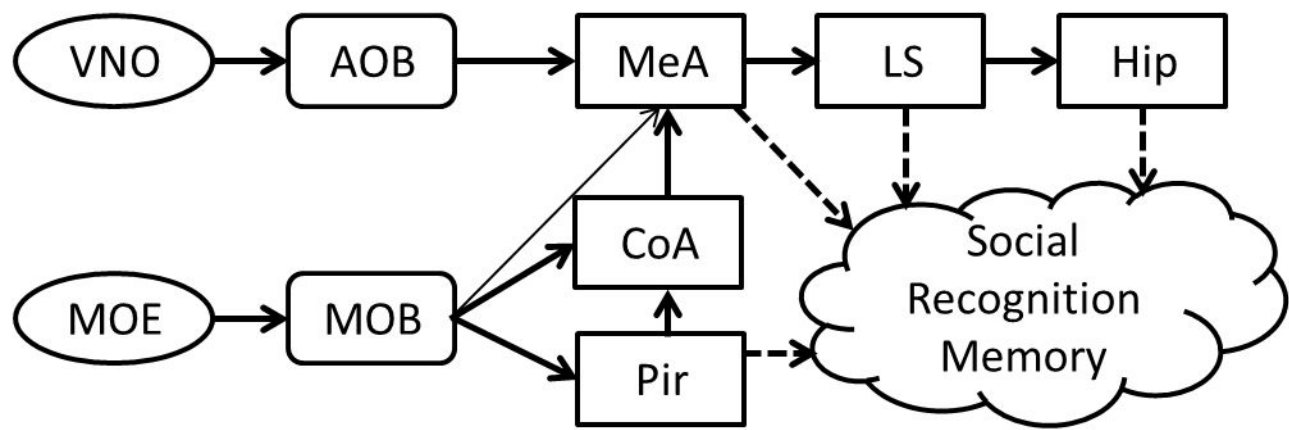
989

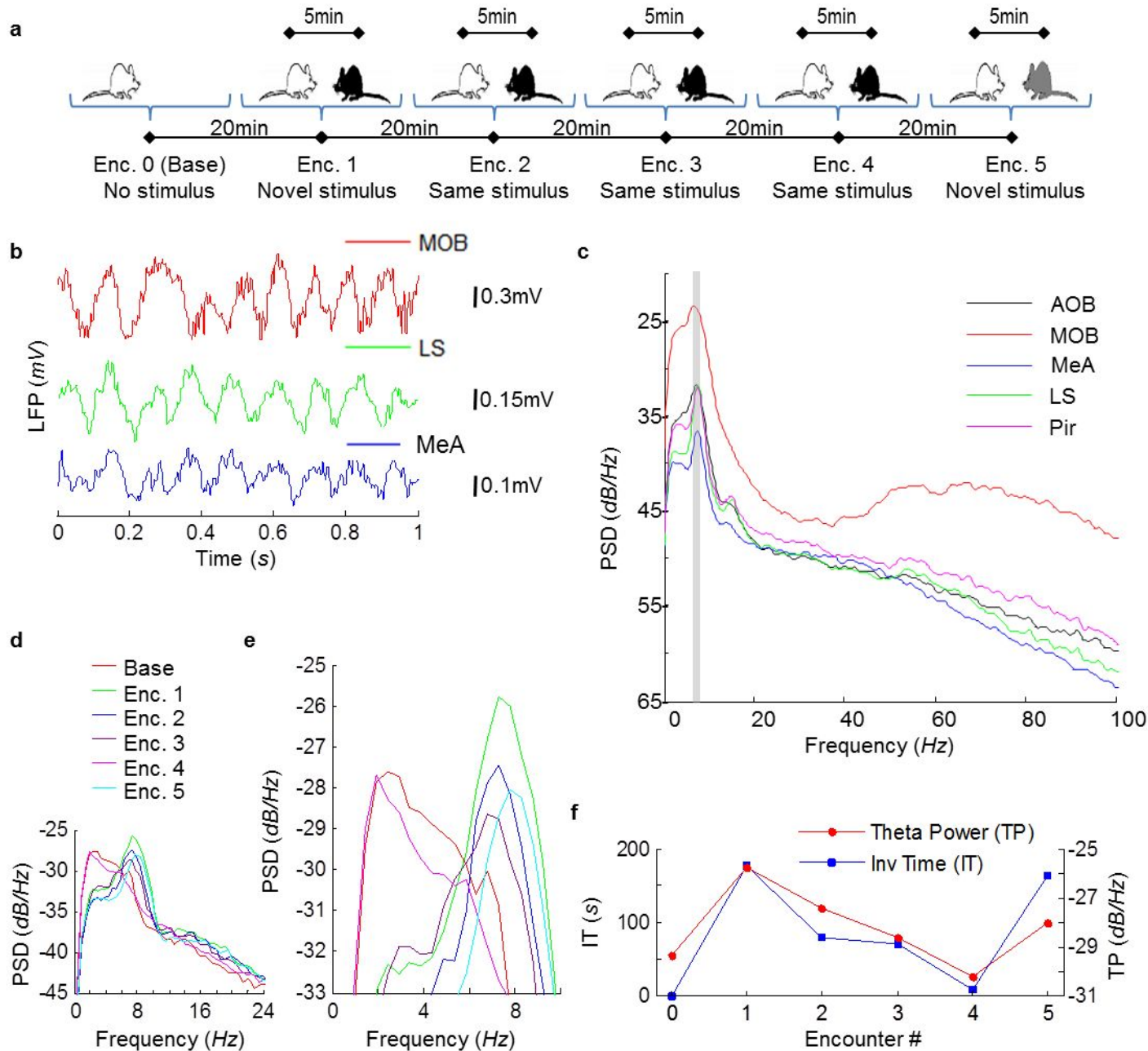
<u>Source data titles and legends</u>	990
Figure 3 – source data 1: Theta power (TP) modulation between encounters.	991
One-way ANOVA (repeated measures) test was used to determine whether there is a	992
significant difference between the mean Δ TP of all 5 encounters during either social	993
(1a) or object (1b) recognition. The assumption of normality was assessed by	994
Lilliefors and Shapiro-Wilk tests. Sphericity was assessed by Mauchly's test.	995
	996
Figure 3 – source data 2: Statistical assessment of habituation and dishabituation	997
Paired t-tests were used for the social (2a) and object (2b) recognition paradigms, to	998
examine if the differences between Enc.1 and Enc. 4 (habituation), as well as between	999
Enc. 4 and Enc. 5 (dishabituation) are statistically significant. Tests were one-sided	1000
and corrected for multiple comparisons using Bonferroni's correction.	1001
	1002
Figure 4 – source data 1: Comparison of ΔTP between Enc. and Post periods	1003
Paired t-tests were used to compare between the mean Δ TP across Enc. vs. the mean	1004
Δ TP across Post periods. The assumption of normality was assessed by Lilliefors and	1005
Shapiro-Wilk tests.	1006
	1007
Figure 6 – source data 1: Assessment of change in theta Coherence from Base to either Enc. 1 or Post 1	1008
	1009
The change from Base to Enc. 1 (upper) and from Base to Post 1 (lower), in theta	1010
coherence during social recognition between the MeA and all other areas (1a) and	1011
between the MOB and all areas (1b), as well as during object recognition between the	1012
MeA and all other areas (1c), and between the MOB and all areas (1d), was	1013
statistically validated using paired t-tests, corrected for multiple comparisons	1014
(Bonferroni correction). The assumption of normality was assessed by Lilliefors and	1015
Shapiro-Wilk tests.	1016
	1017
Figure 7 – source data 1: Comparison of change in theta power in low and high theta bands between social and fearful stimuli.	1018
	1019
Comparison of the change in theta power between social recognition (SR) and fear	1020
conditioning (FC) at high and low theta ranges, statistically validated using two-way	1021

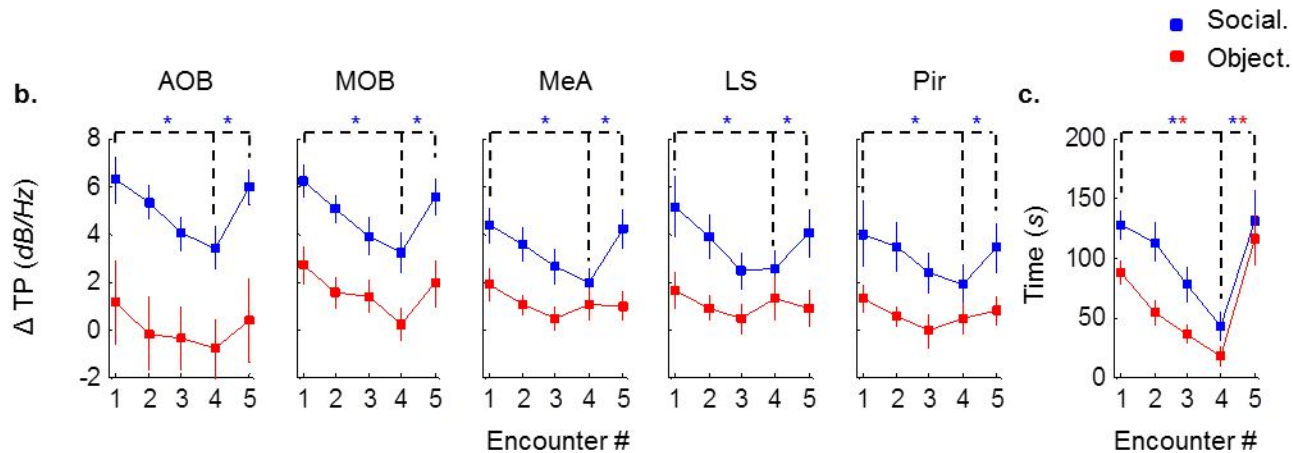
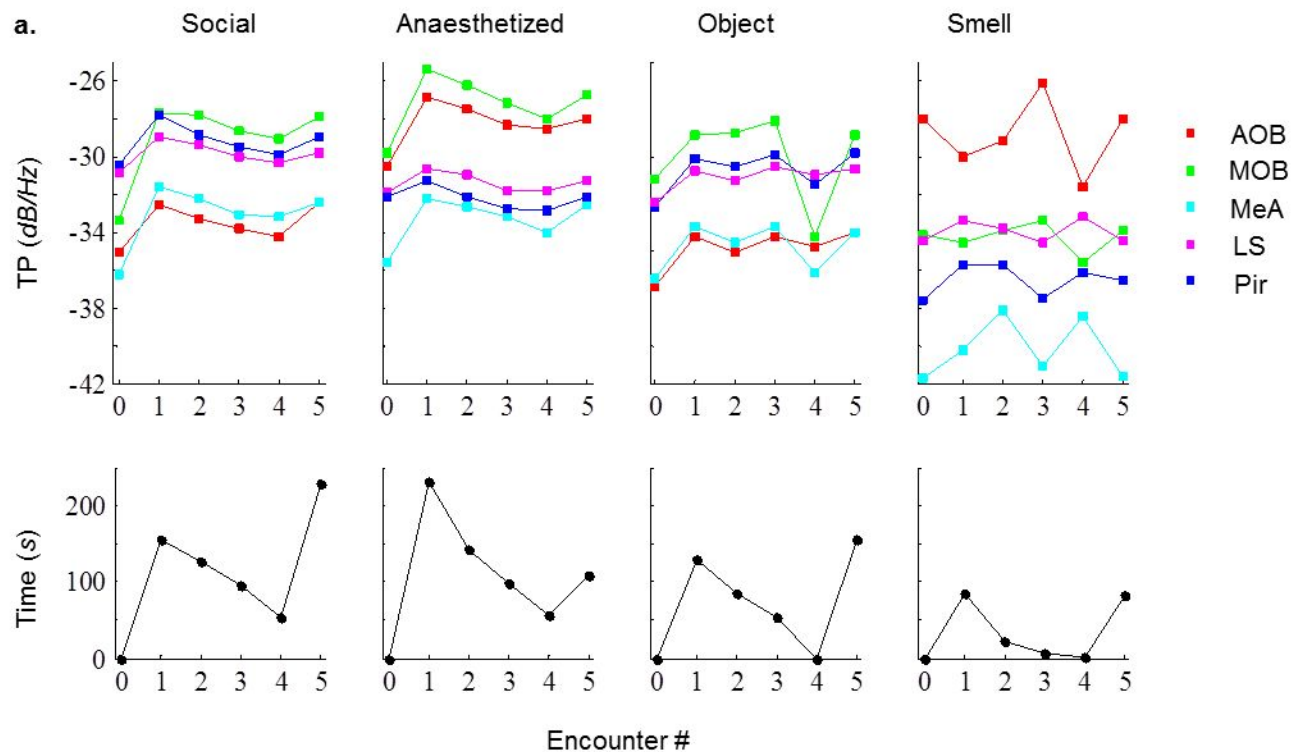
repeated measures ANOVA (p - experiment X theta range interaction). The
assumption of normality was assessed by Lilliefors and Shapiro-Wilk tests.

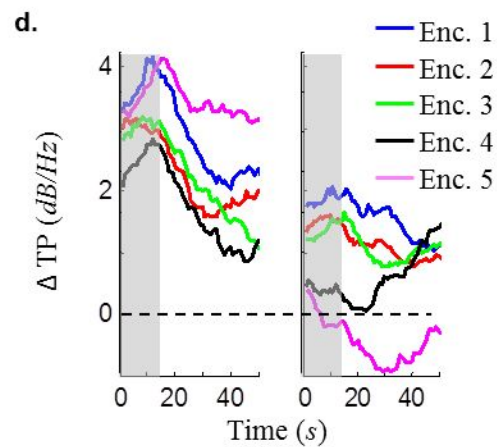
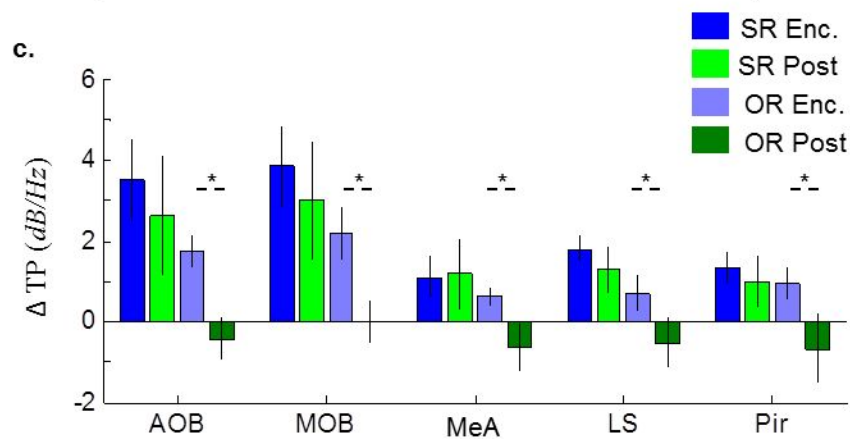
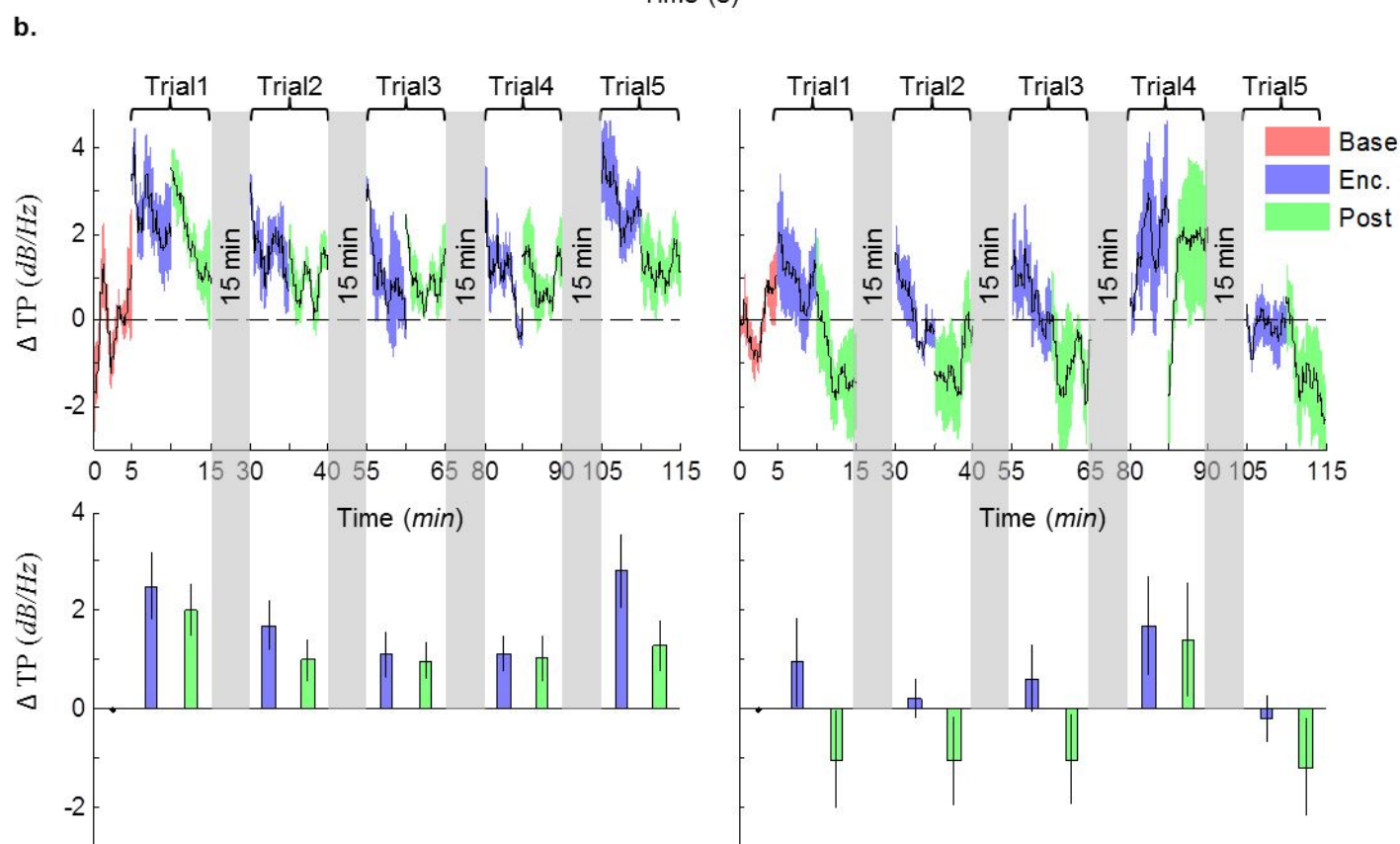
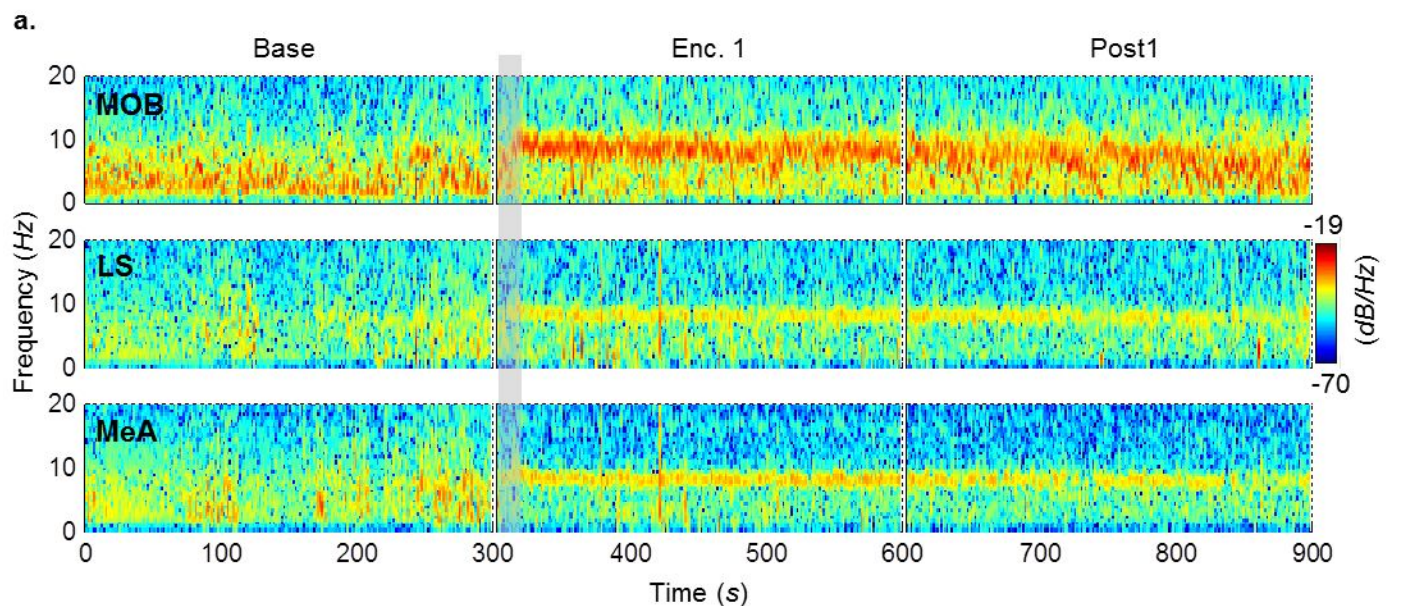
**Figure 8 – source data 1: Comparison of change in coherence in low and high
theta bands between social and fearful stimuli.**

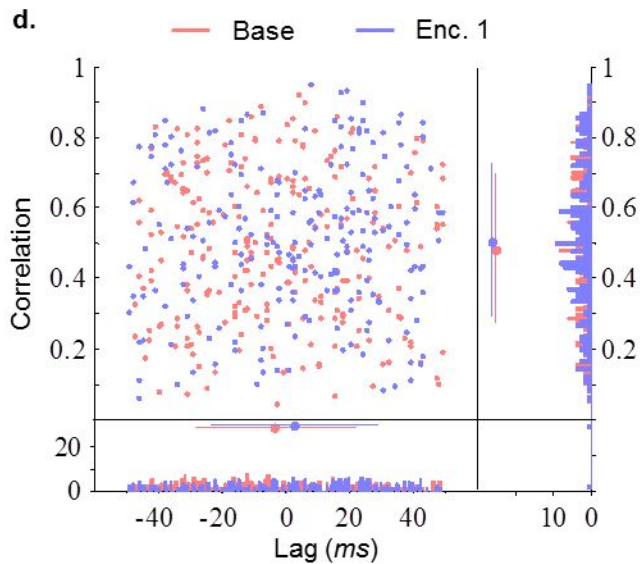
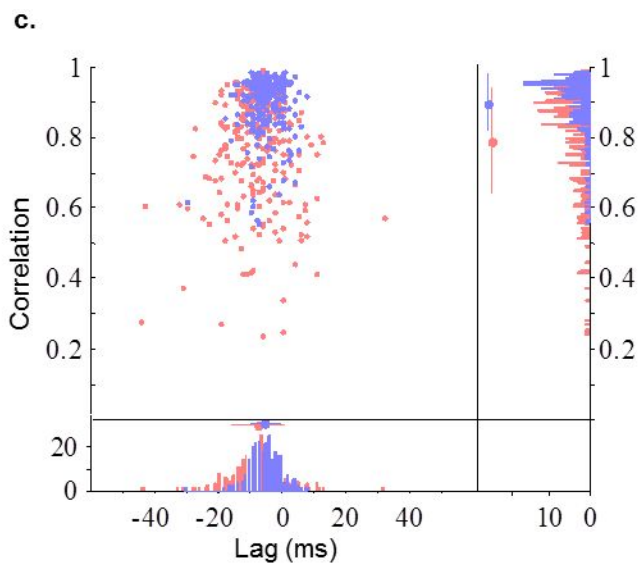
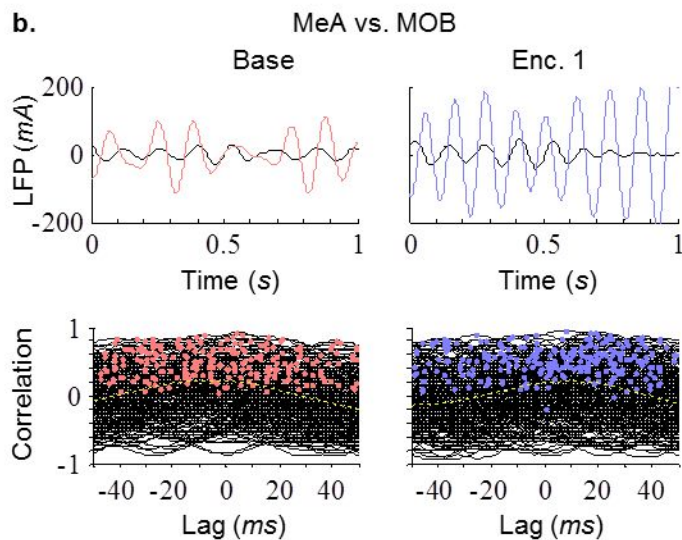
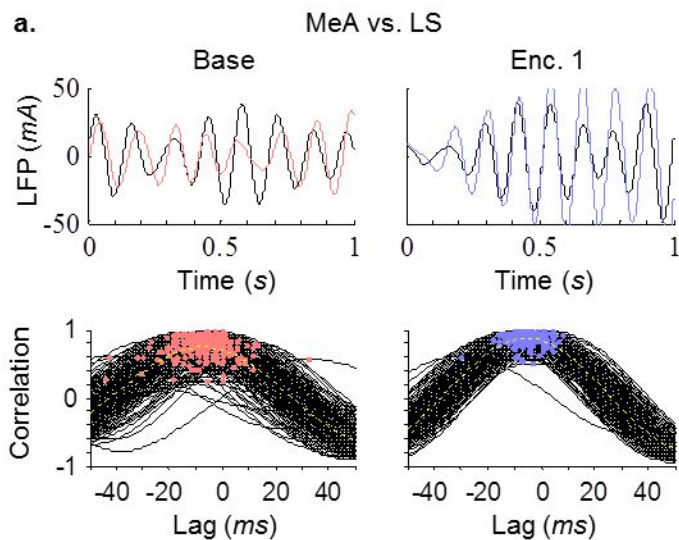
Comparison of the change in coherence between social recognition (SR) and fear
conditioning (FC) at high and low theta ranges (right), statistically validated using
two-way repeated measures ANOVA (p - experiment X theta range interaction). The
assumption of normality was assessed by Lilliefors and Shapiro-Wilk tests.

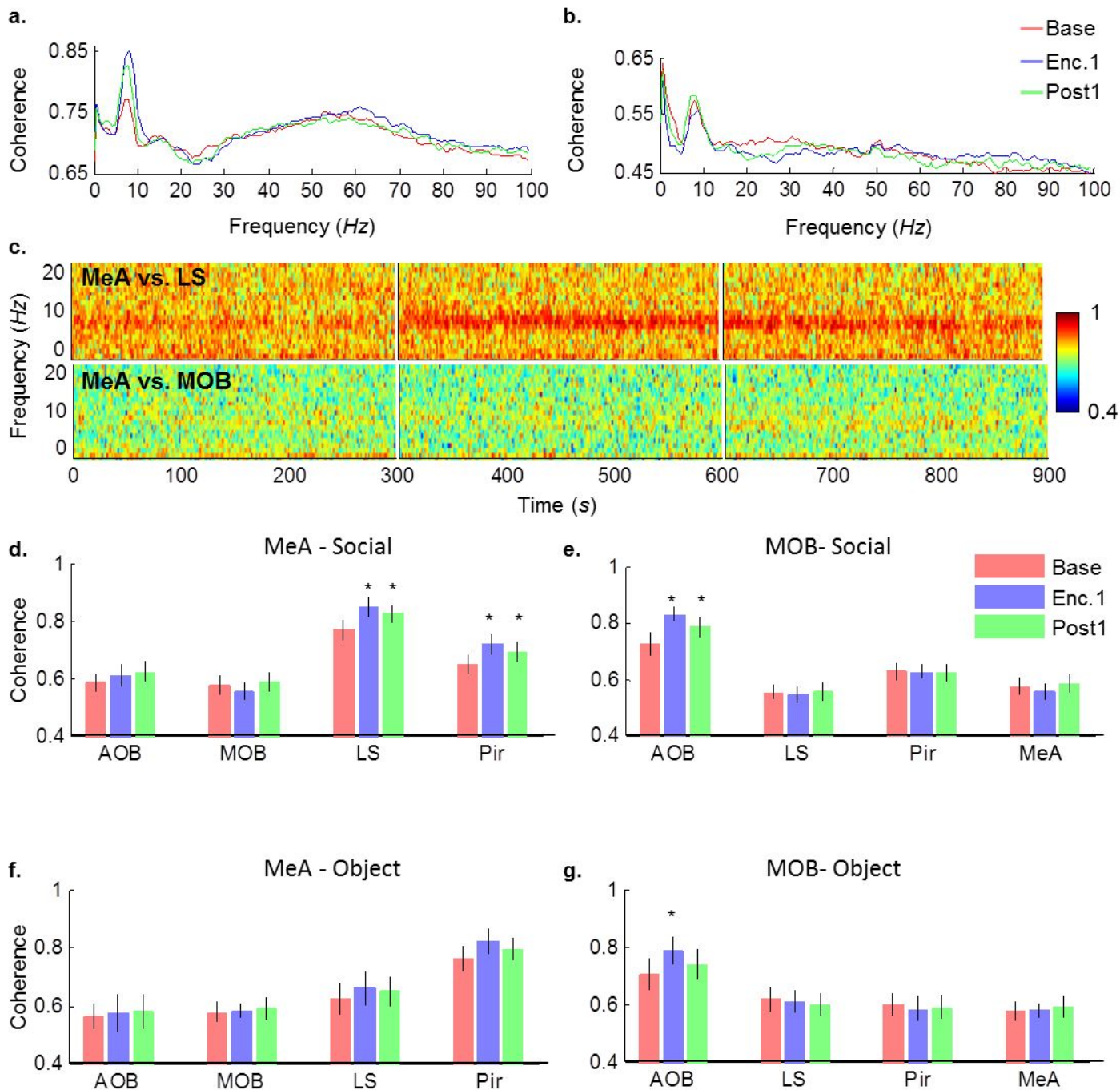


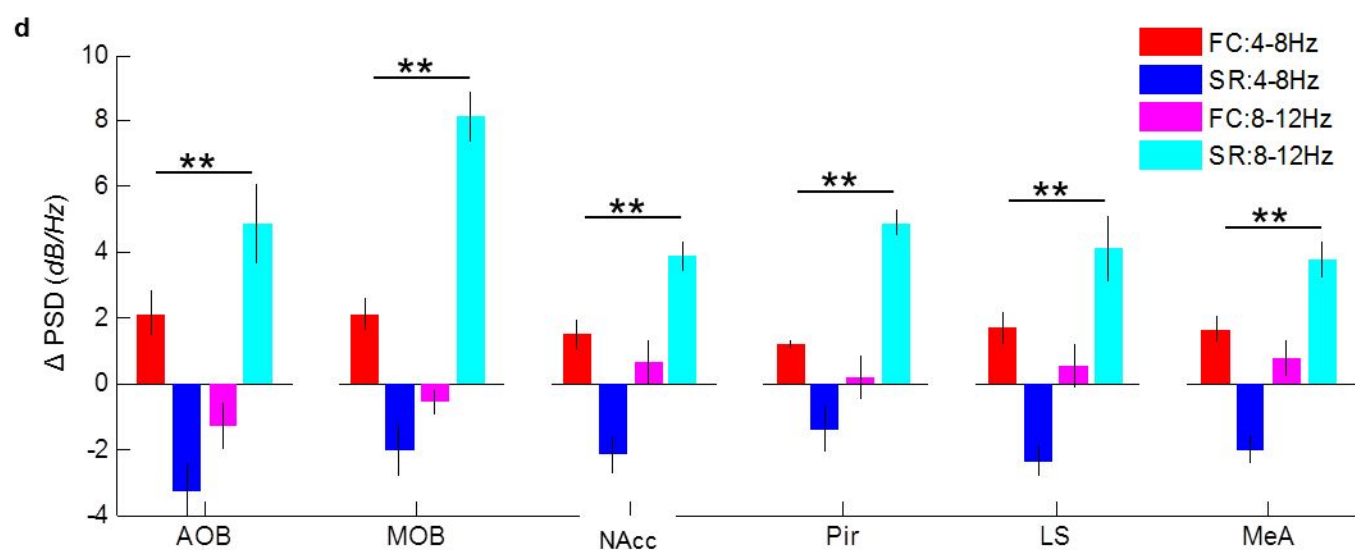
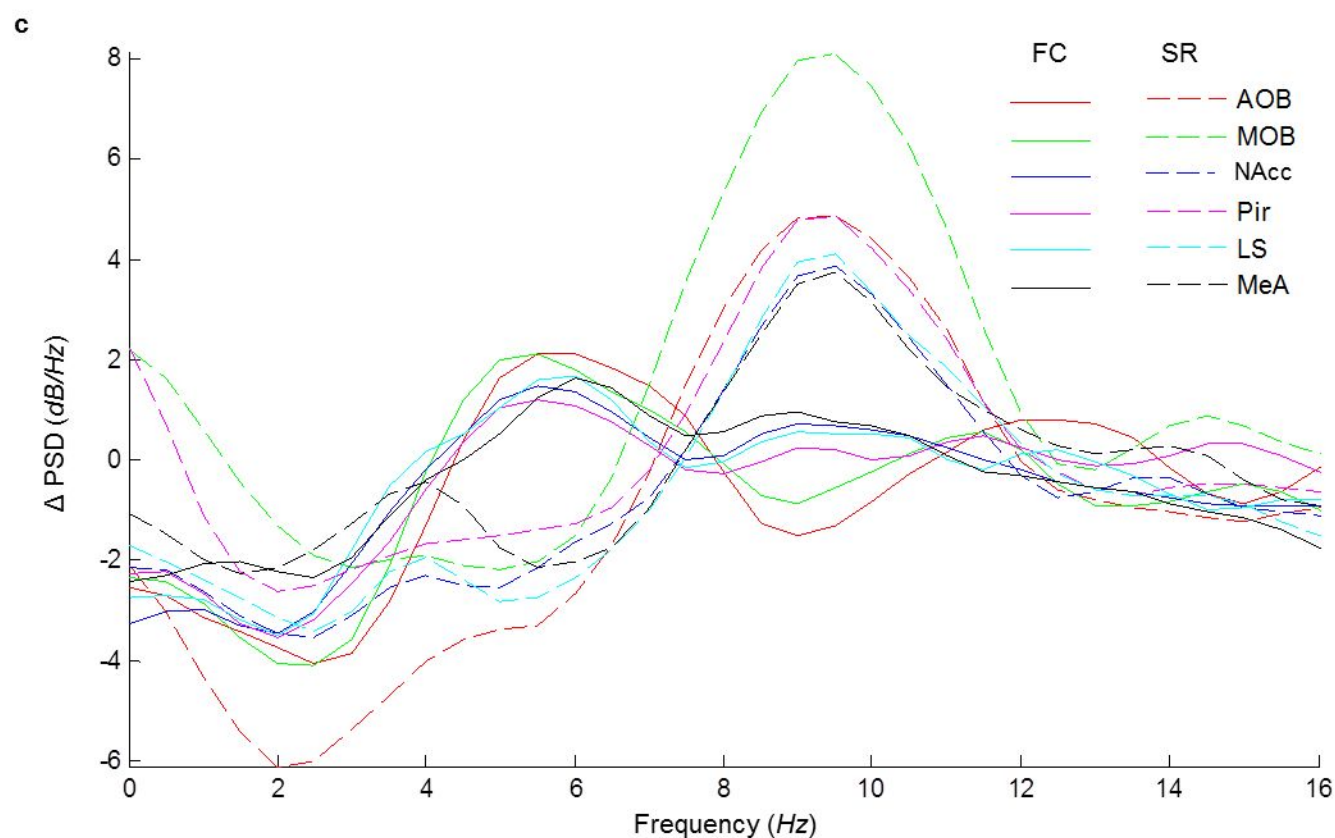
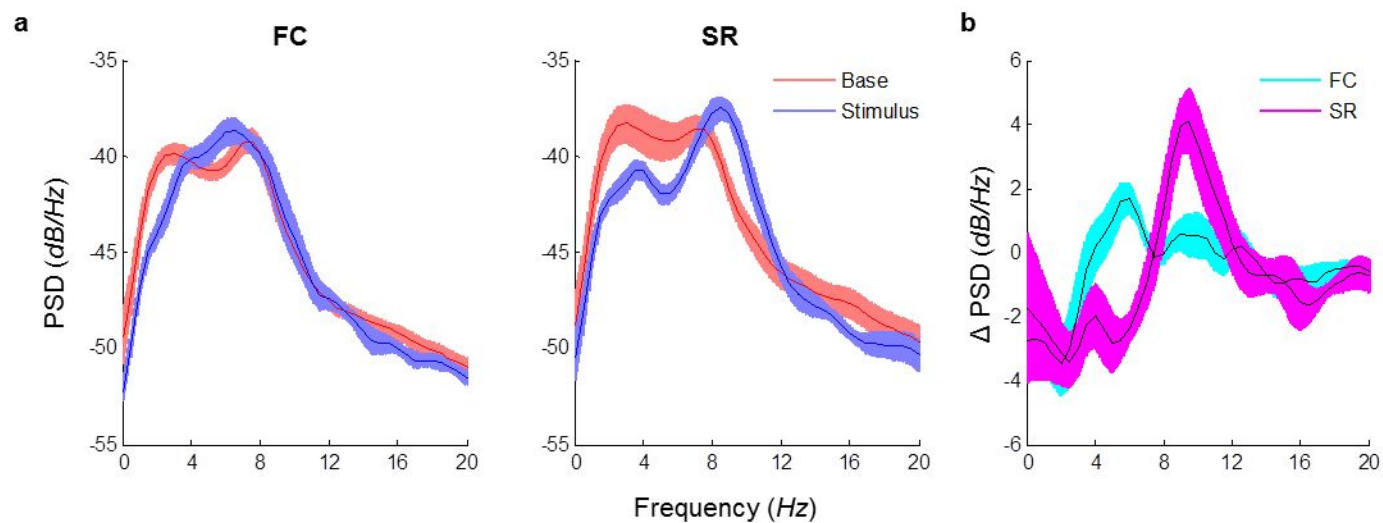




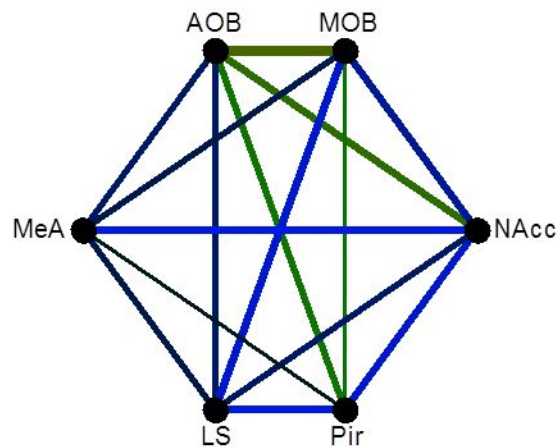




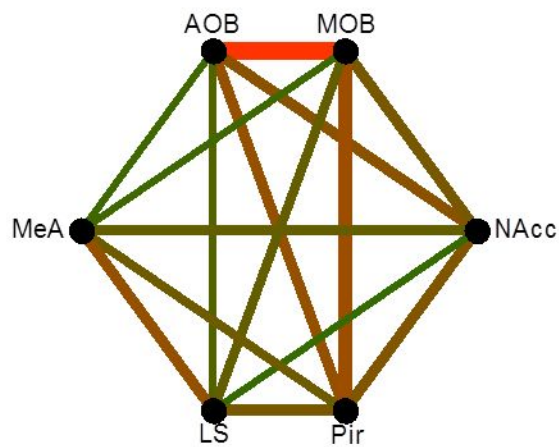




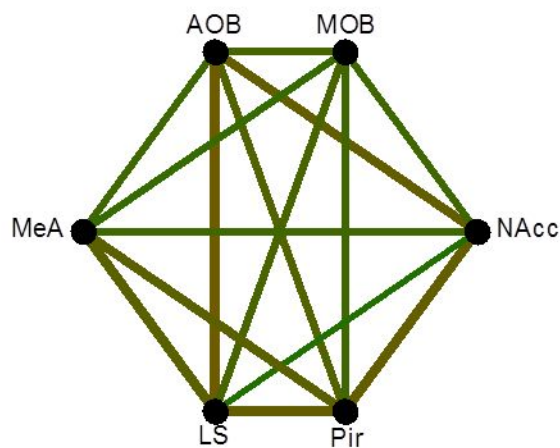
SR: 4-8 Hz



SR: 8-12 Hz



FC: 4-8 Hz



FC: 8-12 Hz

